Supplementary information for

Consistent red luminescence in π-conjugated polymers with tuneable elastic moduli over five orders of magnitude

Zhenfeng Guo,‡[a] Akira Shinohara,‡[a,b] Chengjun Pan,*[a] Florian J. Stadler,*[a] Zhonghua Liu,[a] Zhi-Chao Yan,[a] Jinlai Zhao,[a,c] Lei Wang[a,b] and Takashi Nakanishi*[a,d]

a. *Shenzhen Key Laboratory of Polymer Science and Technology, College of Materials Science and Engineering, Shenzhen University, 1066 Xueyuan Boulevard, Nanshan, Shenzhen 518055, China.*
E-mail: pancj@szu.edu.cn; fjstadler@szu.edu.cn
b. *Key Laboratory of Optoelectronic Devices and Systems of Ministry of Education and Guangdong Province, College of Optoelectronic Engineering, Shenzhen University, 3688 Nanhai Boulevard, Nanshan, Shenzhen 518060, China.*
c. *Faculty of Information Technology, Macau University of Science and Technology, Avenida Wai Long, Taipa, Macau 999078, China.*
d. *International Center for Materials Nanoarchitectonics (WPI-MANA), National Institute for Materials Science (NIMS), 1-1-Namiki, Tsukuba 305-0044, Japan.*
E-mail: NAKANISHI.Takashi@nims.go.jp

Table of Contents

Experimental Procedures **2**

Synthesis **4**

Supplementary Figures **6**

Fig. S1 GPC traces of **P1**–**P4**. 6
Fig. S2 UV–vis absorption and steady-state fluorescence spectra of **P1**–**P4** in toluene 7
Fig. S3 UV–vis absorption and fluorescence spectra of **P1**–**P4** in toluene and in solvent-free state 8
Fig. S4 Fluorescence quantum yields (Φ_{FL}) of **P1**–**P4** in solvent-free state 9
Fig. S5 Fluorescence decay of **P1**–**P4** (a) in solvent-free state and in toluene 10
Fig. S6 Dynamic strain sweeps (DSSs) of **P1**–**P4** 11
Fig. S7 TGA of **P1**–**P4** 12
Fig. S8 DSC traces of **P1**–**P4** 13
Fig. S9 POM image of *n*-dodecyl analogue 14
Fig. S10 DSC traces of **B1**–**B3** 15
Fig. S11 TGA of **B1**–**B3** 16
Fig. S12 Young's modulus mechanical mapping-mode AFM 17
Fig. S13 Fluorescence spectra of **B1**–**B3** in solvent-free state 18
Fig. S14 Dynamic frequency sweeps (DFSs) of **B1**–**B3** 19

Supplementary Tables **20**

Table S1 GPC results of **P1**–**P4** 20
Table S2 Photophysical parameters of **P1**–**P4** in toluene 20
Table S3 TGA summary for **P1**–**P4** 20
Table S4 Peak list details of XRD profiles of **P1**–**P4** 20
Table S5 TGA summary for **B1**–**B3** 21

References **22**

NMR Spectra **23-32**

Experimental Procedures

General

^{1}H and ^{13}C NMR spectra were measured by 16.4 T spectrometer (JEOL) at room temperature in $CDCl_3$. Chemical shifts are expressed in part per million (ppm, δ scale) and are referenced to tetramethylsilane (TMS). Multiplicities are reported as follows: singlet (s), doublet (d), triplet (t), multiplet (m). Gel permeation chromatography (GPC) was performed on a 2695 Separation Module (Waters) equipped with a series of column (Styragel HR 3 and HR 4, 7.8 × 300 mm, calibrated with polystyrene standards, eluent: tetrahydrofuran) and 2414 refractive index (RI) detector (Waters), which was operated at 35 °C. Elemental analysis was conducted by VARIO EL cube (Elementar). All samples were placed in a small boat made of tin foil with a mass of about 2 mg and an error of no more than 0.05 mg. Photos of Alk-CPs were taken by EOS 77D (Canon) equipped with 18-200/F3.6–6.3 Di II VC (B018) (TAMRON) and DG-C Auto Focus Macro Extension Tube (VILTROX). Samples were illuminated by commercial white LED light (Fig. 1b) or handy UV lamp (λ_{max} = ca. 365 nm) (Fig. 1c).

Photophysical characterisation

UV–vis absorption spectra were recorded on either Evolution 220 (Thermo Fischer Scientific) or V-670 (Jasco). The solvent-free samples were prepared by spin coating from toluene solution (10^{-3} mol L^{-1}) onto a glass substrate. Fluorescence spectra were measured on FS5 Fluorescence spectrometer (Edinburgh instruments) (all spectra were corrected). Absolute fluorescence quantum yields (Φ_{FL}) were recorded on Quantaurus C11347 (Hamamatsu Photonics). The difference spectrum between blank and sample gave a negative absorption signal (490–510 nm) and positive emission signal (550–900 nm) (Fig. S4). Φ_{FL} was calculated as the ratio of spectral areas of emission to absorption. Φ_{FL} values are reproducible within 0.4–1.7% (in films) and 0.01–0.2% (in toluene) relative errors, which was confirmed by measuring at least 5 individual samples for each polymer. Fluorescence lifetime was recorded using time-correlated single-photon counting (TCSPC) technique. As an excitation light, NanoLED-390 nanosecond-pulsed diode laser (Horiba) (453 nm, pulse duration <1.4 ns) was used, and the fluorescence was detected by PPD-850 picosecond photon detection module (Horiba).

POM and XRD

Polarised Optical Microscopy (POM) images were captured at room temperature on an ECLIPSE LV100N POL optical microscope (Nikon) equipped with DS-Ri2 CCD camera (Nikon). X-ray diffraction (XRD, λ = 1.5406 nm) measurements were obtained using SmartLab instrument (Rigaku). The samples were placed in Silicon non-diffraction plate for measurements.

Thermal analysis

Thermogravimetric analysis (TGA) was performed with an STA 2500 Regulus (NETZSCH, Selb, Germany) under nitrogen flow (20 mL min^{-1}) at a heating rate of 10 °C min^{-1}. Samples were cast into platinum pan from toluene solution (0.05 mg mL^{-1}) and dried for 6 h at 80 °C under vacuum (p~80 Pa). The weights of samples were ranged 1.42–1.55 mg. Differential scanning calorimetry (DSC) was measured using DSC7020 (Hitachi) with a liquid nitrogen cooling accessory under nitrogen flow (25 mL min^{-1}).

Rheology

Rheology experiments were carried out using a 302 rheometer (Anton Paar), equipped with a parallel plate geometry (4 mm diameter) equipped with a Peltier temperature controller. Firstly, dynamic strain sweep (DSS) measurements were performed to determine the linear viscoelastic range, where G' and G'' are independent from shear strain (γ_0), at an angular frequency (ω) of 1 rad s^{-1} at 25 °C. For the dynamic frequency sweep (DFS) measurement, sufficiently high deformation γ_0 in the linear viscoelastic region were chosen from DSS results, to avoid artefacts (statistical scatter) owing to low torque at low angular frequencies ω.

Force volume (FV) mechanical mapping-mode atomic force microscopy (AFM)

The local elasticity of samples was probed with a commercial AFM Dimension Icon (Bruker) in the Force Volume (FV) mechanical imaging mode. In an FV experiment, a force curve (FC) is obtained by vertically indenting the AFM-tip at every point of a regular matrix in the selected area, which yields the local mechanical response at every point probed. The morphology is reconstructed from the ensemble of the recorded FC, thereby producing a 1:1 correspondence between the morphology and the map of the mechanical properties.

For all measurements, we maintained the total vertical ramp length (L) at 2 µm, selecting a maximum force (F) of ≈280 nN and vertical approaching velocity (v) of ≈20 µm s^{-1}. We performed experiments with 64 × 64 lateral resolution, while 4096 points were acquired for each force curve. A series of 3–4 FV measurements were performed in different macroscopic positions to improve the statistical reliability of the experiments. All samples were imaged in air at room temperature (25 °C).

We used a standard sharp indenter model TAP 150A (Bruker) with averaged semi-angle aperture = 17°. The elastic spring constant, k = 2.7 N m^{-1}, was calibrated in air using the Sader method.[S1] Young's moduli (E) were evaluated by data analysis performed in a Matlab (Math-works) environment with a routine fully described in Galluzzi et al.[S2,S3] Briefly, for each FV

measurement, single force curves were pre-processed to obtain force curves (F [nN]) vs. indentation (δ). The total indentation length was added to the untreated morphology in order to obtain the uncompressed morphology. After pre-treatment, the indentation curves are fitted using the Sneddon model for sharp probes:[S4,S5]

$$F = 0.7453 \left(E \tan\vartheta \, \delta^2/(1-\nu^2)\right)$$

where E, ν, ϑ, and δ represent the local Young's modulus, the Poisson ratio and the averaged half-opening angle of the indenter, and indentation, respectively. We used logarithmic Young's moduli values to build the mechanical map and the collective histogram for statistical analysis. For a single FV measurement, the error associated must take this calibration error and the variability of Young's moduli in the FV-area, i.e., the width of log-normally distributed values, into account. The final error characteristics depend on the error of a single force volume and its variation due to measurements in different macroscopic locations on the same sample.

Synthesis

Chemicals

Alkyl bromides and potassium carbonate were purchased from Energy Chemicals (China). 2,5-Dibromohydroquinone and 4,7-bis(2-trimethylstannyl-4-hexyl-2-thienyl)-2,1,3-benzothiadiazole were obtained from Alfa Chemicals (China). Tris(dibenzylideneacetone)dipalladium(0) and tri(*o*-tolyl)phosphine were obtained from Green Chemicals (China). Solvent for reactions included *N*,*N*-dimethylformamide and chlorobenzene (anhydrous, Energy Chemicals).

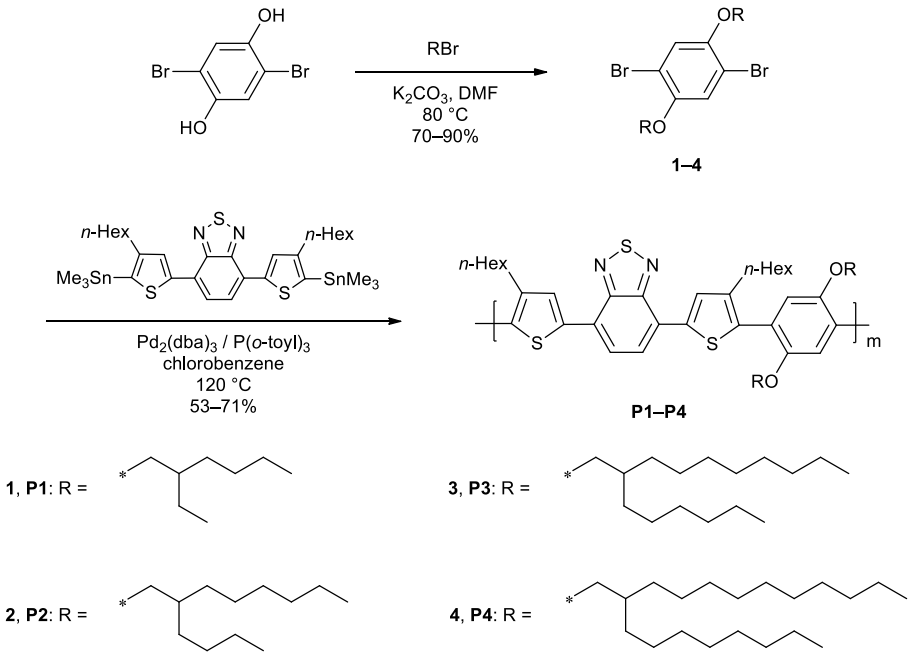

Scheme S1. Synthetic route to **P1**–**P4**.

General method for synthesis of monomers. One equivalent 2,5-dibromohydroquinone, 2.5 equivalents alkyl bromide and 10 equivalents potassium carbonate were placed in a 100 mL two-neck flask. The flask was evacuated and refilled with nitrogen. Proper anhydrous *N*,*N*-dimethylformamide was injected via syringe and the mixture was stirred for 24 h at 80 °C. The reaction mixture was diluted with dichloromethane and sequentially washed with 1 mol L^{-1} hydrochloric acid (1×), water (3×) and brine (1×). The organic layer was dried over magnesium sulphate and concentrated under reduced pressure. The residue was purified by column chromatography on silica gel with *n*-hexane as eluent to obtain desired compounds. Yields were ranged 70–90%.

1,4-Dibromo-2,5-bis(2-ethylhexyloxy)benzene (1):[S6] Colourless liquid. T_g (DSC): −72.2 °C. ^{1}H NMR (700 MHz): δ/ppm 0.90–0.95 (m, 12H, CH_3), 1.26–1.57 (m, 16H, CH_2), 1.74 (m, 2H, CH), 3.83 (m, 4H, O–CH_2), 7.08 (s, 2H, benzene). ^{13}C NMR (176 MHz): δ/ppm 11.16, 14.09, 23.03, 23.87, 29.04, 30.45, 39.42, 72.51, 111.05, 118.16, 150.16.
1,4-Dibromo-2,5-bis(2-butyloctyloxy)benzene (2):[S7] Colourless liquid. T_g (DSC): −73.9 °C. ^{1}H NMR (700 MHz): δ/ppm 0.84–0.95 (m, 12H, alkyl), 1.24–1.54 (m, 32H, alkyl), 1.65–1.80 (m, 2H, alkyl), 3.82 (d, J = 5.6 Hz, 4H, O–CH_2), 7.07 (s, 2H, benzene). ^{13}C NMR (176 MHz): δ/ppm 14.09, 14.13, 22.69, 23.04, 26.79, 29.03, 29.67, 31.00, 31.31, 31.84, 37.94, 72.92, 111.04, 118.17, 150.16.
1,4-Dibromo-2,5-bis(2-hexyldecyloxy)benzene (3):[S8] Colourless liquid. T_g (DSC): −82.0 °C. ^{1}H NMR (700 MHz): δ/ppm 0.84–0.92 (m, 12H, alkyl), 1.22–1.51 (m, 48H, alkyl), 1.76–1.82 (m, 2H, alkyl), 3.82 (d, J = 5.6 Hz, 4H, O–CH_2), 7.07 (s, 2H, benzene). ^{13}C NMR (176 MHz): δ/ppm 14.3, 22.69, 26.79, 26.81, 29.34, 29.58, 29.67, 30.00, 31.30, 31.31, 31.85, 31.92, 37.95, 72.93, 111.04, 118.17, 150.16 [14 of 16 alkyl peaks were observed owing to overlap of peaks].
1,4-Dibromo-2,5-bis(2-octyldodecyloxy)benzene (4):[S9] Colourless liquid. T_g (DSC): −73.4 °C. M. p. (DSC): 14.9 °C. ^{1}H NMR (700 MHz): δ/ppm 0.81–0.93 (t, 12H, alkyl), 1.20–1.53 (m, 64H, alkyl), 1.74–1.84 (m, 2H, alkyl), 3.82 (d, J = 5.6 Hz, 4H, O–CH_2), 7.07 (s, 2H, benzene). ^{13}C NMR (176 MHz): δ/ppm 14.13, 22.70, 22.71, 26.82, 29.35, 29.37, 29.58, 29.62, 29.66, 29.68, 30.00, 31.30, 31.93, 31.94, 37.95, 72.93, 111.05, 118.16, 150.16 [16 of 20 alkyl peaks were observed owing to overlap of peaks].

Note that T_g of **4** is higher than that of **3**. In addition, **4** exhibited a crystalline feature with melting point of 14.9 °C while compound **1**–**3** are amorphous over the measurement conditions. This phenomenon is probably due to the larger van der

Waals attraction force than perturbation and repulsive forces for **4**. Therefore, **3** showed the lowest T_g among the four monomers. Indeed, such unusual T_g trend is also found in other reported alkyl–π compounds by our group.[S10,S11]

General method for the Stille cross-coupling polymerisation. One equivalent the monomer (**1**–**5**), 1 equivalent 4,7-bis(2-trimethylstannyl-4-hexyl-2-thienyl)-2,1,3-benzothiadiazole, 0.25 equivalent tri(*o*-tolyl)phosphine and 0.05 equivalent tris(dibenzylideneacetone)dipalladium(0) were added into the 50 mL two-neck flask. The flask was evacuated and refilled with nitrogen several times. Proper anhydrous chlorobenzene was injected via syringe, and the mixture was stirred at 110 °C for 72 h. The reaction mixture was diluted with dichloromethane and washed with water (3×) and brine (1×) sequentially. The organic layer was dried over magnesium sulphate and concentrated under reduced pressure. The residue was reprecipitated from tetrahydrofuran/acetone (× 3) and then dichloromethane/methanol (1×). The precipitate was dried under vacuum at room temperature overnight to obtain desired polymers. Yields were ranged from 53–71%.

Poly[(2,5-bis(2-ethylhexyloxy)benzene-1,4-diyl)-*alt*-(4-hexylthiophene-2,5-diyl)(2,1,3-benzothiadiazole-4,7-diyl)(3-hexylthiophene-2,5-diyl)] (P1): Dark red solid (0.246 g, 53%). Number-average molecular weight (M_n) = 9.5 kg mol^{-1}, polydispersity index (PDI) = 1.21. ^{1}H NMR (700 MHz): δ/ppm 0.61–0.97 (18H, alkyl), 1.15–1.76 (34H, alkyl), 2.52–2.77 (4H, alkyl), 3.69–3.96 (4H, O–CH_2), 7.04 (2H, benzene), 7.75–7.91 (2H, thiophene), 8.01–8.11 (2H, benzothiazole).^{13}C NMR (176 MHz): δ/ppm 11.13, 14.06, 14.15, 22.70, 23.07, 23.89, 29.05, 29.28, 29.40, 30.59, 30.82, 31.76, 39.57, 72.21, 117.12, 124.18, 125.14, 125.83, 129.10, 135.28, 137.85, 141.67, 150.77, 152.77. Anal. Calcd for $C_{48}H_{66}N_2O_2S_3$: C, 72.13; H, 8.32; N, 3.50; S, 12.04. Found: C, 70.37; H, 7.62; N, 3.42; S, 12.04.

Poly[(2,5-bis(2-butyloctyloxy)benzene-1,4-diyl)-*alt*-(4-hexylthiophene-2,5-diyl)(2,1,3-benzothiadiazole-4,7-diyl)(3-hexylthiophene-2,5-diyl)] (P2): Dark red rubber (0.268 g, 55%). M_n = 9.7 kg mol^{-1}, PDI = 1.21. ^{1}H NMR (700 MHz): δ/ppm 0.65–0.93 (18H, alkyl), 1.06–1.81 (48H, alkyl), 2.57–2.74 (4H, alkyl), 3.75–3.90 (4H, O–CH_2), 6.96–7.07 (2H, benzene), 7.73–7.92 (2H, thiophene), 7.99–8.12 (2H, benzothiazole). ^{13}C NMR (176 MHz): δ/ppm 14.05, 14.06, 14.15, 22.68, 22.70, 23.07, 26.87, 29.07, 29.28, 29.40, 29.78, 30.81, 31.15, 31.50, 31.77, 31.87, 38.15, 72.71, 117.16, 124.23, 125.07, 128.81, 129.10, 135.25, 137.84, 141.68, 150.80, 152.75.Anal. Calcd for $C_{56}H_{82}N_2O_2S_3$: C, 73.80; H, 9.07; N, 3.07; S, 10.55. Found: C, 74.26; H, 8.41; N, 3.09; S, 10.81.

Poly[(2,5-bis(2-hexyldecyloxy)benzene-1,4-diyl)-*alt*-(4-hexylthiophene-2,5-diyl)(2,1,3-benzothiadiazole-4,7-diyl)(3-hexylthiophene-2,5-diyl)] (P3): Dark red tar-like liquid (0.408 g, 71%). M_n =10.0 kg mol^{-1}, PDI = 1.35. ^{1}H NMR (700 MHz): δ/ppm 0.73–0.93 (18H, alkyl), 1.06–1.76 (66H, alkyl), 2.57–2.75 (4H, alkyl), 3.71–3.90 (4H, O–CH_2), 7.01–7.05 (2H, benzene), 7.84–7.90 (2H, thiophene), 8.05–8.11 (2H, benzothiazole). ^{13}C NMR (176 MHz): δ/ppm 14.05, 14.11, 14.16, 22.68, 22.70, 26.87, 26.92, 29.29, 29.40, 29.65, 29.78, 30.14, 30.80, 31.50, 31.77, 31.87, 31.90, 38.18, 72.75, 117.21, 124.26, 125.05, 125.81, 129.13, 135.25, 137.84, 141.68, 150.81, 152.75 [19 of 22 alkyl peaks were observed owing to overlap of peaks]. Anal. Calcd for $C_{64}H_{98}N_2O_2S_3$: C, 75.09; H, 9.65; N, 2.74; S, 9.40. Found: C, 75.41; H, 9.09; N, 2.69; S, 9.55.

Poly[(2,5-bis(2-octyldodecyloxy)benzene-1,4-diyl)-*alt*-(4-hexylthiophene-2,5-diyl)(2,1,3-benzothiadiazole-4,7-diyl)(3-hexylthiophene-2,5-diyl)] (P4): Dark red viscous liquid (0.622 g, 70%). M_n = 12.0 kg mol^{-1}, PDI = 1.31. ^{1}H NMR (700 MHz): δ/ppm 0.77–0.92 (18H, alkyl), 1.06–1.74 (82H, alkyl), 2.45–2.81 (4H, alkyl), 3.74–3.86 (4H, O–CH_2–), 6.77–7.12 (2H, benzene), 7.76–7.94 (2H, thiophene), 8.00–8.17 (2H, benzothiazole). ^{13}C NMR (176 MHz): δ/ppm 14.11, 14.13, 14.16, 22.68, 22.70, 26.93, 29.29 29.37. 29.41, 29.65, 29.70, 29.75, 30.14, 30.80, 31.50, 31.78, 31.90, 31.93, 38.18, 72.76, 117.22, 124.27, 125.04, 125.82, 129.11, 135.23, 137.84, 141.67, 150.80, 152.76 [20 of 26 alkyl peaks were observed owing to overlap of peaks]. Anal. Calcd for $C_{72}H_{114}N_2O_2S_3$: C, 76.13; H, 10.12; N, 2.47; S, 8.47. Found: C, 76.24; H, 9.45; N, 2.40; S, 8.49.

Supplementary Figures

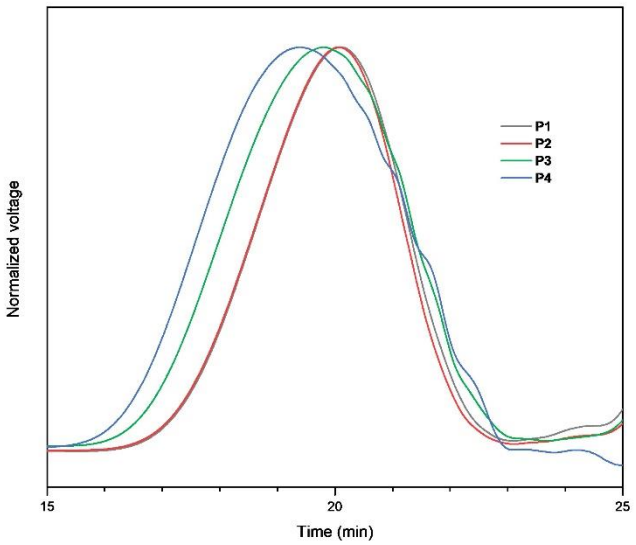

Fig. S1 GPC traces of **P1**–**P4**. M_w, M_n, polydispersity index (PDI), and degree of polymerisation (m) are summarised in Table S1.

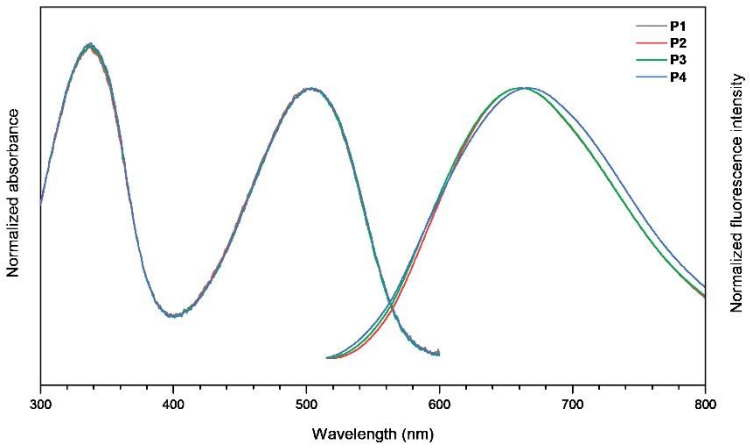

Fig. S2 UV–vis absorption and steady-state fluorescence spectra of **P1**–**P4** in toluene. Concentration: 10^{-5} mol L^{-1} (absorption); 10^{-6} mol L^{-1} (fluorescence). Excitation wavelength: 365 nm.

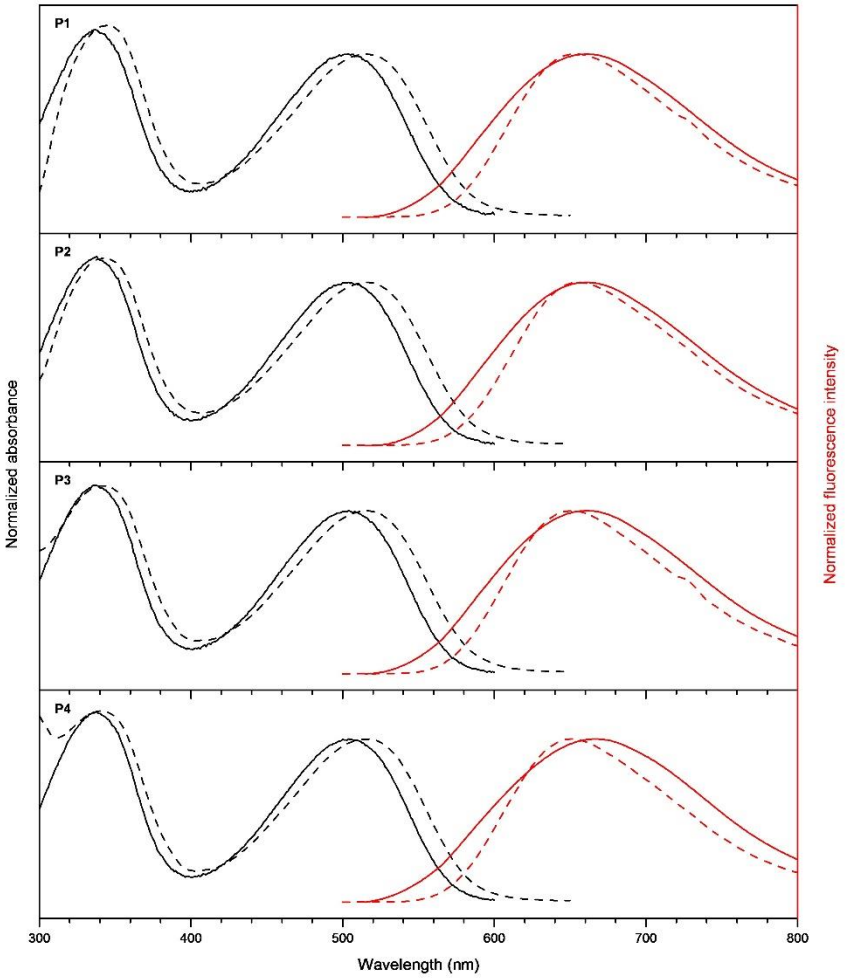

Fig. S3 UV–vis absorption and fluorescence spectra of **P1**–**P4** in toluene (solid line) and in solvent-free state (dashed line). Excitation wavelength: 365 nm.

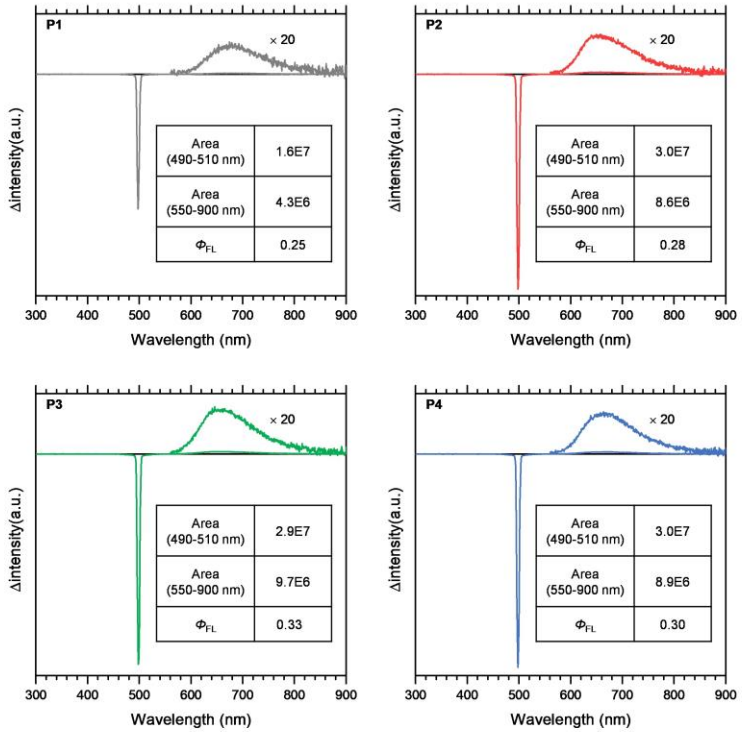

Fig. S4 Fluorescence quantum yields (Φ_{FL}) of **P1**–**P4** in solvent-free state. Excitation wavelength: 500 nm.

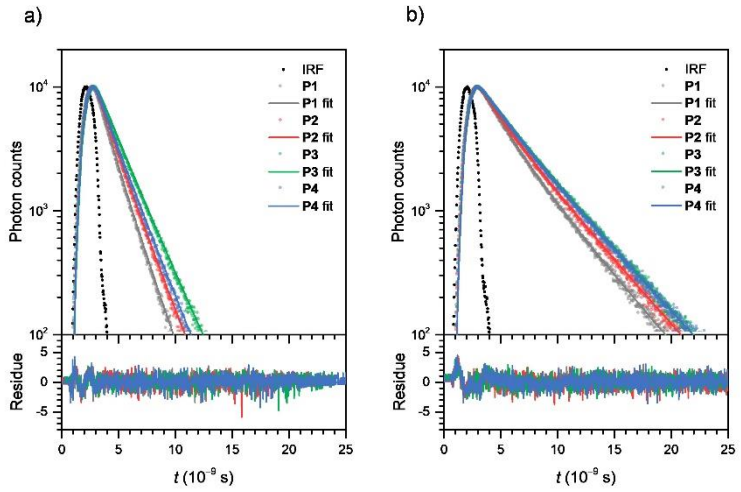

Fig. S5 Fluorescence decay of **P1**–**P4** (a) in solvent-free state and (b) in toluene (10^{-6} mol L^{-1}). Excitation wavelength: 453 nm. Monitoring wavelength: 650 nm. Two decay components were required to give a reasonable fit, as judged by the chi-square value (χ^2) being between 0.8 and 1.2. The fluorescence decay parameters are summarised in Table 1 (solvent-free) and Table S2 (in toluene). IRF: instrument response function.

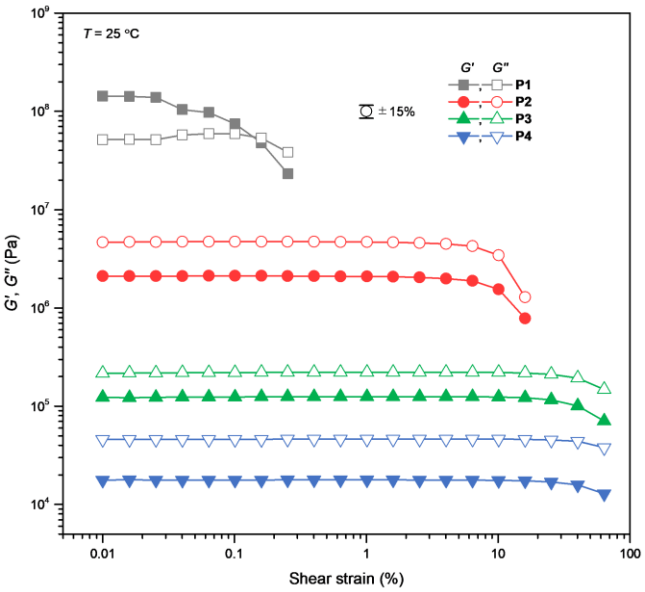

Fig. S6 Dynamic strain sweeps (DSSs) of **P1**–**P4** at angular frequency ω = 1 rad s^{-1}. Error bar = ±15%.

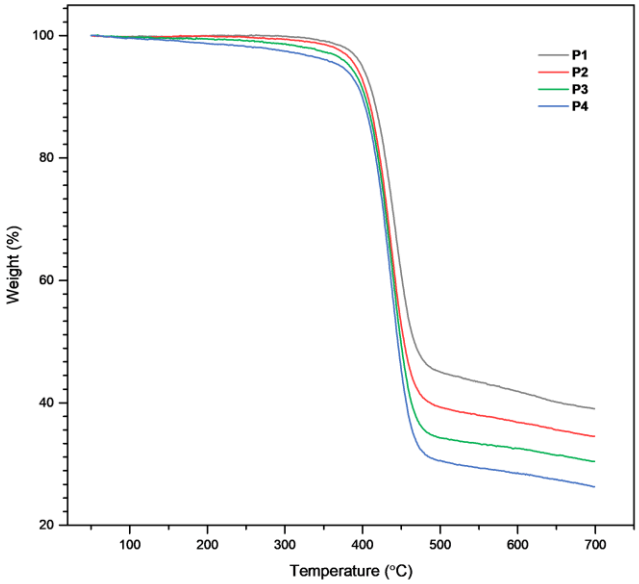

Fig. S7 TGA profiles of **P1**–**P4**.

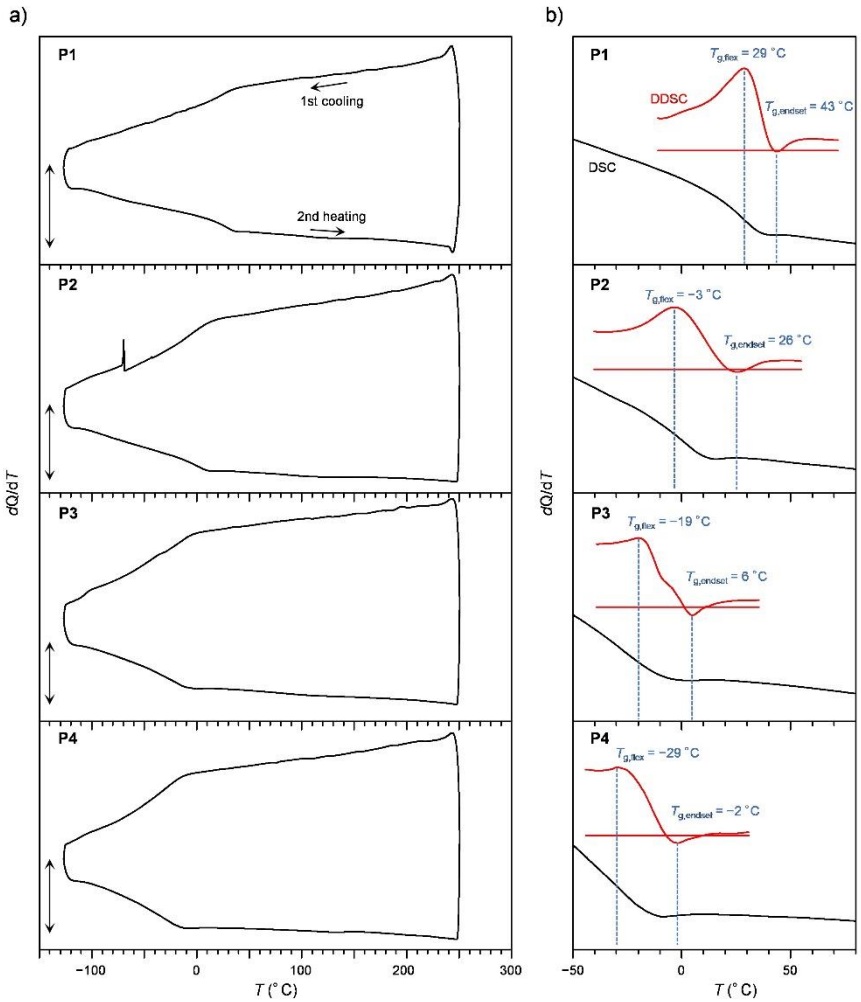

Fig. S8 DSC traces of **P1**–**P4**. (a) First cooling and second heating traces. Double arrows represent 1 mW. (b) Magnification of the glass transition region in the second heating trace. Sample weight: 4.10 mg (**P1**); 3.98 mg (**P2**); 4.90 mg (**P3**); 4.91 mg (**P4**).

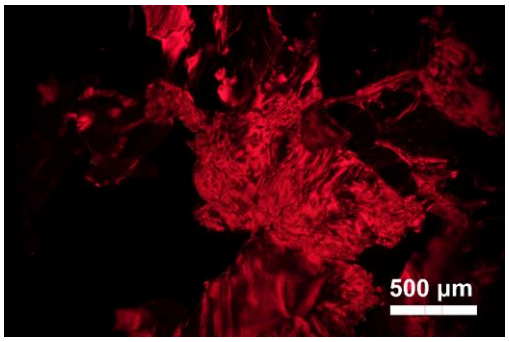

Fig. S9 POM image of *n*-dodecyl analogue.

A *n*-dodecyl analogue of Alk-CP was synthesised from in the same manner as **P1**–**P4**.

1,4-Dibromo-2,5-bis(dodecyloxy)benzene:[S12] White solid, ^{1}H NMR (700 MHz): δ/ppm 0.87–0.90 (t, 6H, alkyl), 1.21–1.82 (m, 40H, alkyl), 3.92–3.97 (t, J = 6.6 Hz, 4H, O–CH_2), 7.08 (s, 2H, benzene). ^{13}C NMR (176 MHz): δ/ppm 14.13, 22.70, 25.93, 29.12, 29.30, 29.36, 29.55, 29.58, 29.65, 29.66, 29.93, 31.93, 70.31, 111.12, 118.46, 150.07 T_m (DSC): 81.0 °C.

Poly(2,5-bis(dodecyloxy)benzene-1,4-diyl)-*alt*-(4-hexylthiophene-2,5-diyl)(2,1,3-benzothiadiazole-4,7-diyl)(3-hexylthiophene-2,5-diyl)] (*n*-dodecyl analogue): Dark red solid (0.201 g, 57%). M_n = 9.0 kg mol^{-1}, PDI = 1.39. ^{1}H NMR (700 MHz): δ/ppm 0.79–0.92 (12H, alkyl), 1.09–1.77 (56H, alkyl), 2.43–2.73 (4H, alkyl), 3.75–4.08 (4H, O–CH_2), 6.84–7.09 (2H, benzene), 7.76–7.92 (2H, thiophene), 8.02–8.13 (m, 2H, benzothiazole). ^{13}C NMR (176 MHz): δ/ppm 14.13, 22.69, 26.09, 29.33, 29.36, 29.38, 29.61, 29.63, 29.66, 29.70, 30.73, 31.66, 31.78, 31.91, 69.78, 117.24, 125.19, 129.24, 135.22, 137.89, 141.70, 150.49, 152.75 [15 of 18 alkyl peaks were observed owing to overlap of peaks. 8 of 10 aromatic peaks were observed owing to overlap of peaks]. Anal. Calcd for $C_{56}H_{82}N_2O_2S_3$: C, 73.80; H, 9.07; N, 3.07; S, 10.55. Found: C, 72.38; H, 8.279; N, 2.86; S, 10.008.

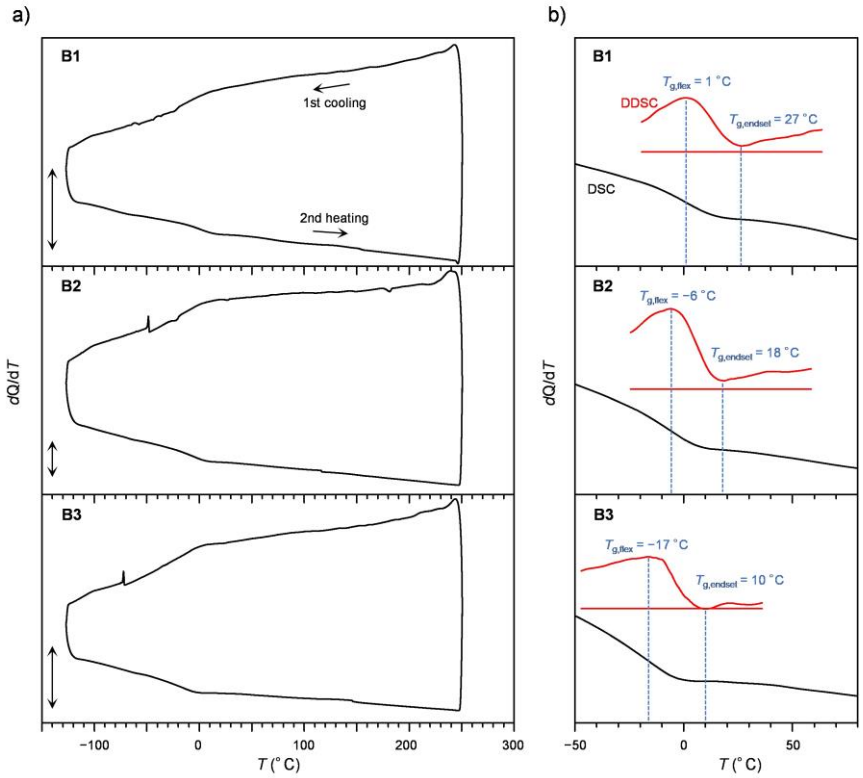

Fig. S10 DSC traces of **B1**–**B3**. (a) First cooling and second heating traces. Double arrows represent 1 mW. (b) Magnification of the glass transition region in the second heating trace. Sample weight: 3.13 mg (**B1**); 6.64 mg (**B2**); 4.08 mg (**B3**).

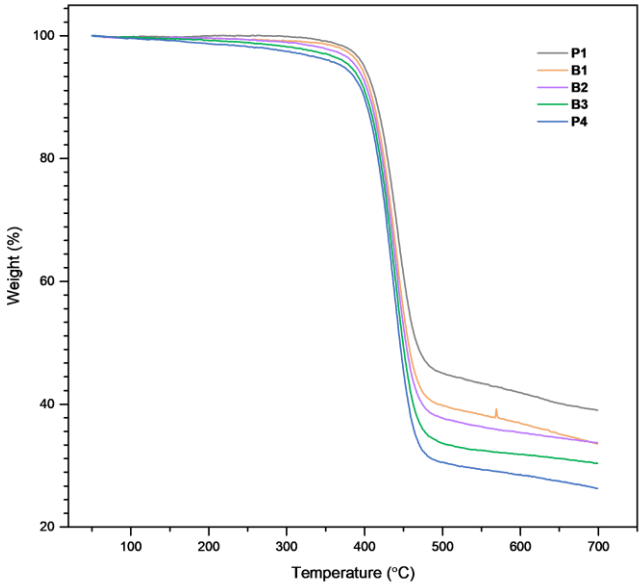

Fig. S11 TGA profiles of **P1**, **B1**–**B3**, and **P4**.

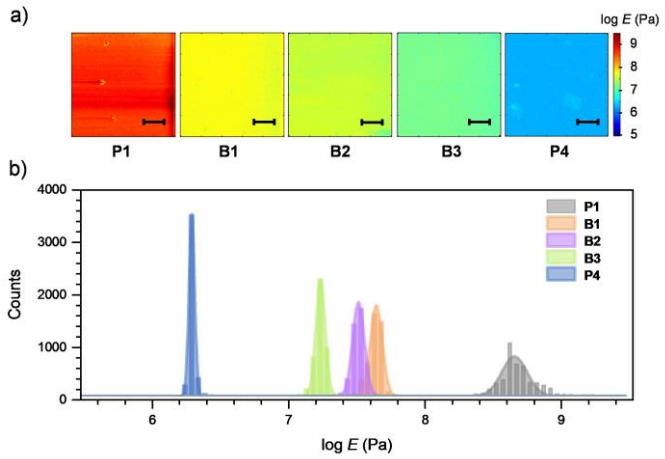

Fig. S12 (a) Young's modulus mechanical mapping-mode AFM images of **B1**–**B3**. Scale bar = 2 µm. (b) Histograms of Young's modulus values (*E*) in log-normal scale with a Gaussian distribution fit.

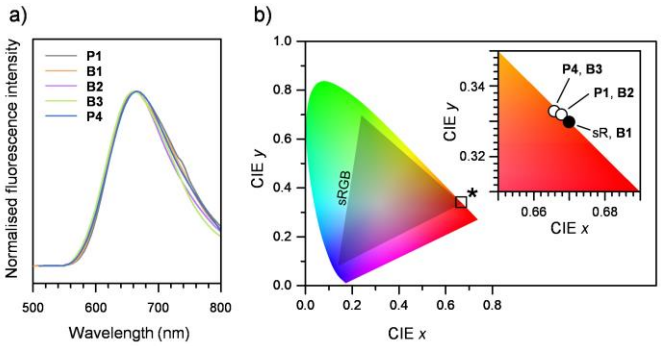

Fig. S13 Fluorescence spectra of **B1**–**B3** in solvent-free state. CIE chromaticity coordinates (*x*, *y*) = (0.670, 0.330) (**B1**); (0.668, 0.332) (**B2**); (0.666, 0.333) (**B3**).

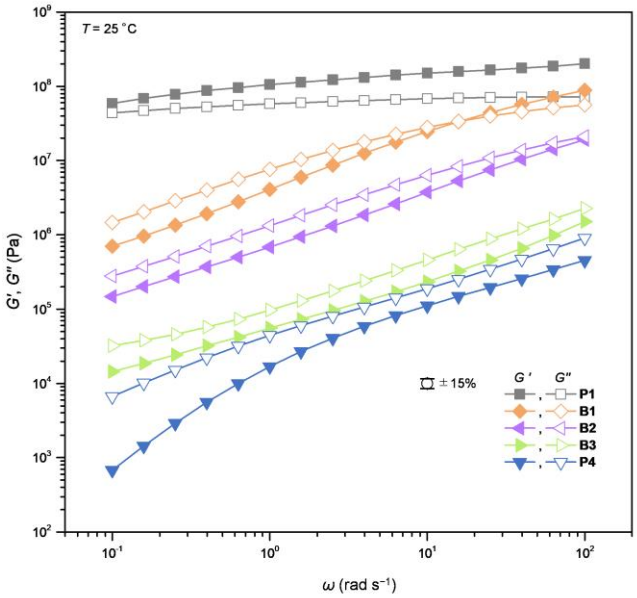

Fig. S14 Dynamic frequency sweeps (DFSs) of **B1**–**B3** at shear amplitude (γ_0) = 0.1% (**B1**); 1.0% (**B2**); 3.0% (**B3**). Error bar = ±15%.

Supplementary Tables

Table S1 GPC results of **P1**–**P4**.

Polymer	M_w[a] (kg mol^{-1})	M_n[b] (kg mol^{-1})	PDI[c]	M.W. of repeating unit[d] (g mol^{-1})	m[e]
P1	12.0	9.5	1.21	799	11.9
P2	12.0	9.7	1.26	911	10.6
P3	14.0	10.0	1.35	1024	9.8
P4	16.0	12.0	1.31	1136	10.6

[a] Weight-averaged molecular weight. [b] Number-averaged molecular weight. [c] Polydispersity index (= M_w/M_n). [d] Molecular weight of repeating unit (i.e. DTBT unit + dialkoxyphenylene unit). [e] Number-average degree of polymerisation (= M_n/(M.W. of repeating unit)).

Table S2 Photophysical parameters of **P1**–**P4** in toluene.

Polymer	τ_1 (ns)	A_1[a]	τ_2 (ns)	A_2[a]	τ_{ave}[b] (ns)	Φ_{FL}[c]	k_R[d] (10^8 s^{-1})	k_{NR}[e] (10^8 s^{-1})
P1	2.06	0.40	4.17	0.60	3.32	0.59	1.78	1.23
P2	2.21	0.30	4.30	0.70	3.68	0.68	1.85	0.87
P3	2.47	0.22	4.37	0.78	3.96	0.75	1.90	0.63
P4	2.56	0.33	4.57	0.67	3.91	0.72	1.84	0.72

[a] Amplitude of decay component. [b] Amplitude-weighted average lifetime. Excitation wavelength: 453 nm. Monitoring wavelength: 650 nm. [c] Absolute fluorescence quantum yield. Excitation wavelength: 500 nm. [d] Radiative decay rate constants $k_R = \Phi_{FL}/\tau_{ave}$. [e] Non-radiative decay rate constants $k_{NR} = (1 - \Phi_{FL})/\tau_{ave}$.

Table S3 TGA summary for **P1**–**P4**.

Polymer	$T_{99\%}$[a] (°C)	$T_{95\%}$[b] (°C)
P1	358	400
P2	332	392
P3	273	376
P4	172	355

[a] 1% weight loss temperature. [b] 5% weight loss temperature.

Table S4 Peak list details of XRD profiles of **P1**–**P4**.

Polymer	2ϑ (°)	d (nm)
P1	5.03	1.76
	21.3	0.42
P2	4.76	1.86
	20.8	0.43
P3	4.67	1.89
	20.2	0.44
P4	4.63	1.91
	20.1	0.44

Table S5 TGA summary for **B1**–**B3** as well as **P1** and **P4** as the comparison.

Polymer /blend	$T_{99\%}$[a] (°C)	$T_{95\%}$[b] (°C)
P1	358	400
B1	323	395
B2	296	390
B3	240	382
P4	172	355

[a] 1% weight loss temperature. [b] 5% weight loss temperature.

References

S1 J. E. Sader, J. W. M. Chon and P. Mulvaney, *Rev. Sci. Instrum.*, 1999, **70**, 3967–3969.

S2 M. Galluzzi, G. Tang, C. S. Biswas, J. Zhao, S. Chen and F. J. Stadler, *Nat. Commun.*, 2018, **9**, 3584.

S3 M. Galluzzi, C. S. Biswas, Y. Wu, Q. Wang, B. Du and F. J. Stadler, *NPG Asia Mater.*, 2016, **8**, e327.

S4 I. N. Sneddon, *Int. J. Eng. Sci.*, 1965, **3**, 47–57.

S5 G. G. Bilodeau, *J. Appl. Mech.*, 1992, **59**, 519–523.

S6 Y. Lyu, D. Cui, J. Huang, W. Fan, Y. Miao and K. Pu, *Angew. Chem. Int. Ed.*, 2019, **58**, 4983–4987.

S7 H. Um, J. Lee, H. Baik, M. Cho and D. Choi, *Chem. Commun.*, 2016, **52**, 13012–13015.

S8 N. S. Gobalasingham, J. E. Carlé, F. C. Krebs, B. C. Thompson, E. Bundgaard and M. Helgesen, *Macromol. Rapid Commun.*, 2017, **38**, 1700526.

S9 C. Roy, T. Bura, S. Beaupré, M. A. Légaré, J. P. Sun, I. G. Hill and M. Leclerc, *Macromolecules*, 2017, **50**, 4658–4667.

S10 F. Lu, K. Jang, I. Osica, K. Hagiwara, M. Yoshizawa, M. Ishii, Y. Chino, K. Ohta, K. Ludwichowska, K. J. Kurzydłowski, S. Ishihara and T. Nakanishi, *Chem. Sci.*, 2018, **9**, 6774−6778.

S11 B. Narayan, K. Nagura, T. Takaya, K. Iwata, A. Shinohara, H. Shinmori, H. Wang, Q. Li, X. Sun, H. Li, S. Ishihara and T. Nakanishi, *Phys. Chem. Chem. Phys.*, 2018, **20**, 2970−2975.

S12 X. Maimaitiyiming, A. Abodurexiti and N.Dongmulati, *Mater. Chem. Phys.*, 2020, **40**, 122116.

NMR spectra

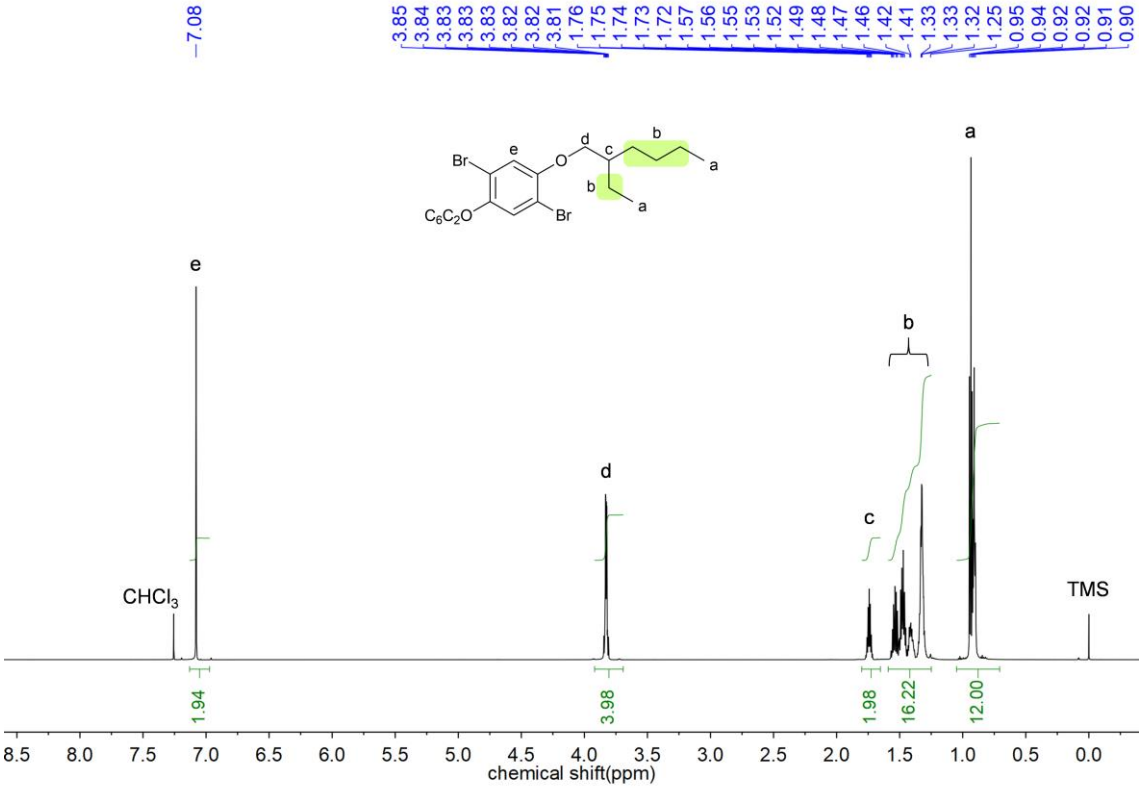

^{1}H NMR (700 MHz) spectrum of **1**.

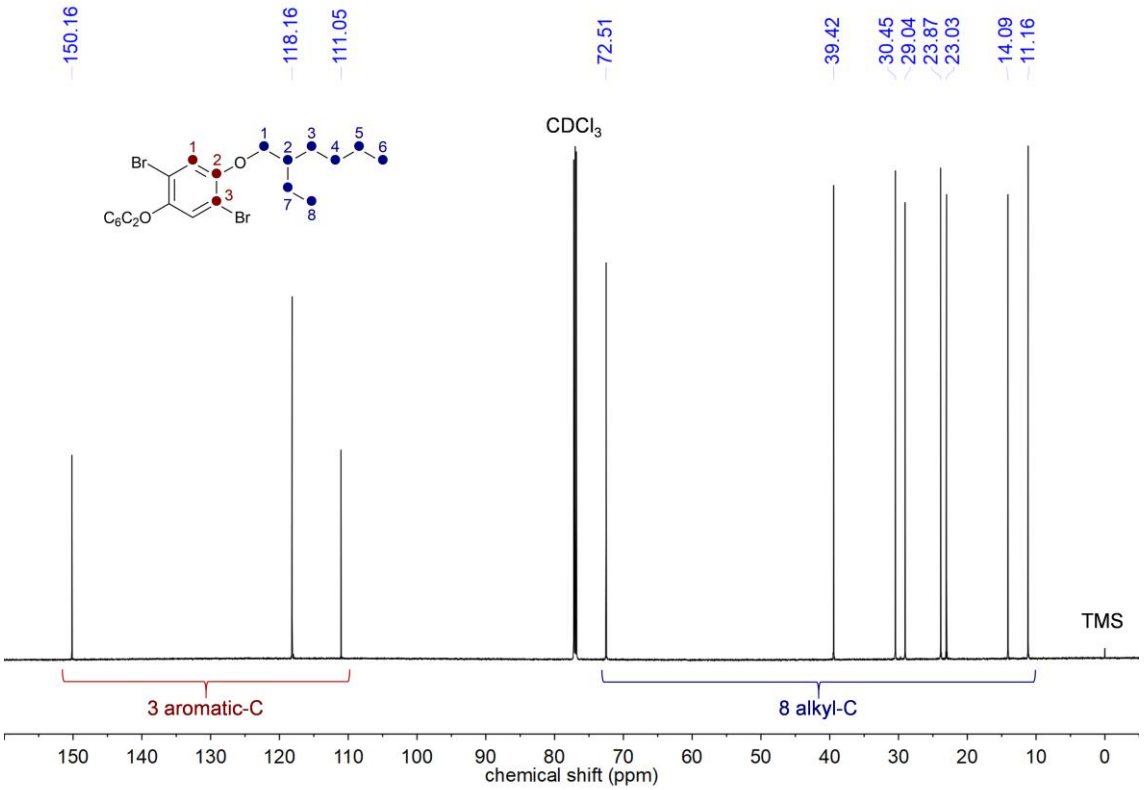

^{13}C NMR (176 MHz) spectrum of **1**.

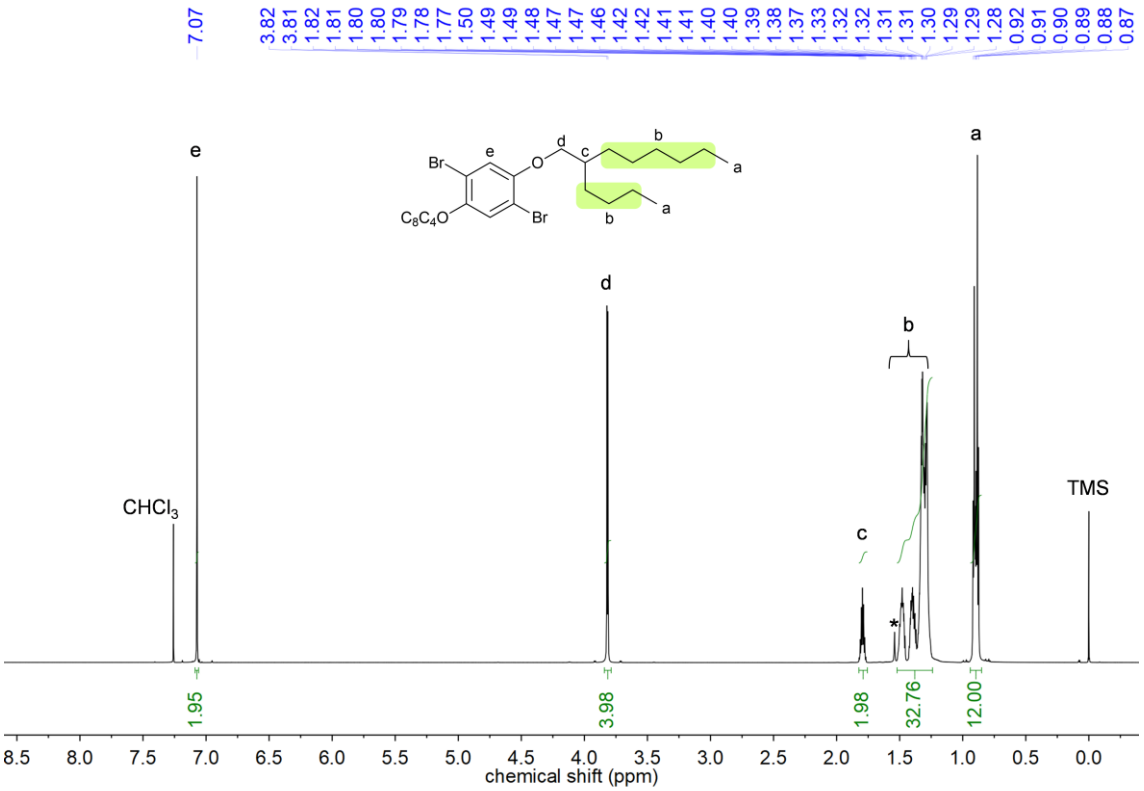

^{1}H NMR (700 MHz) spectrum of **2**. The asterisk represents residual water.

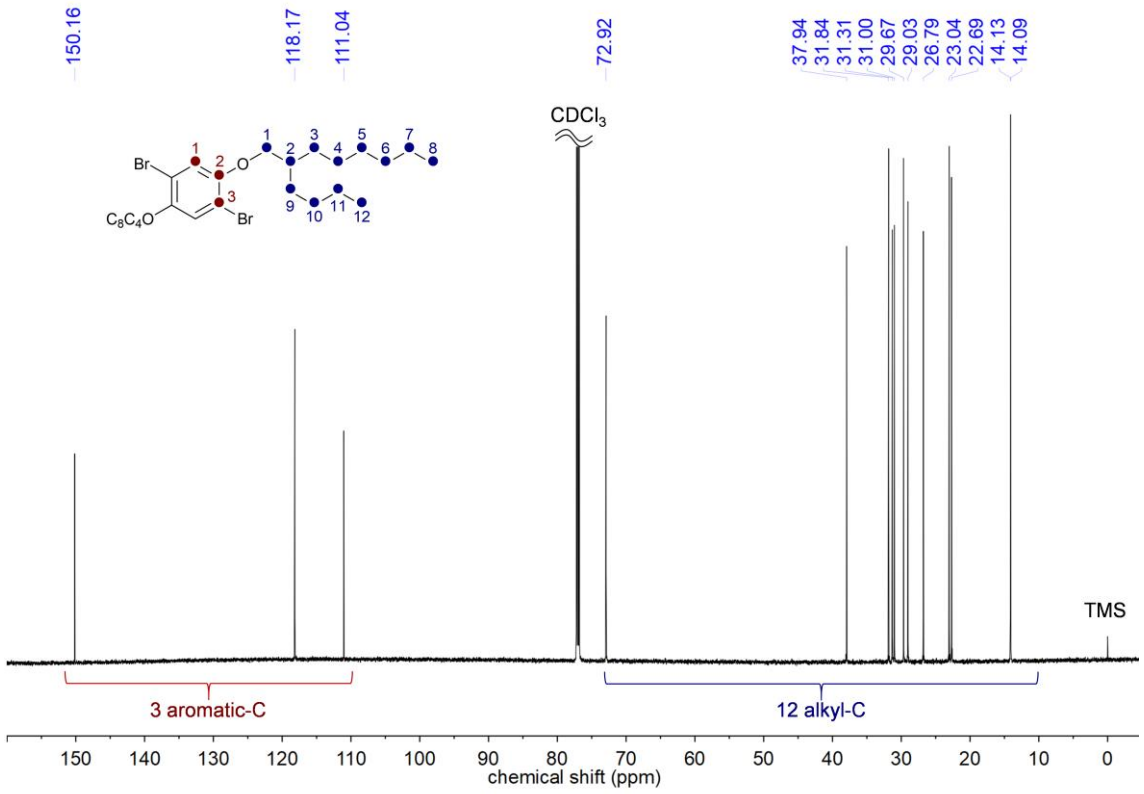

^{13}C NMR (176 MHz) spectrum of **2**.

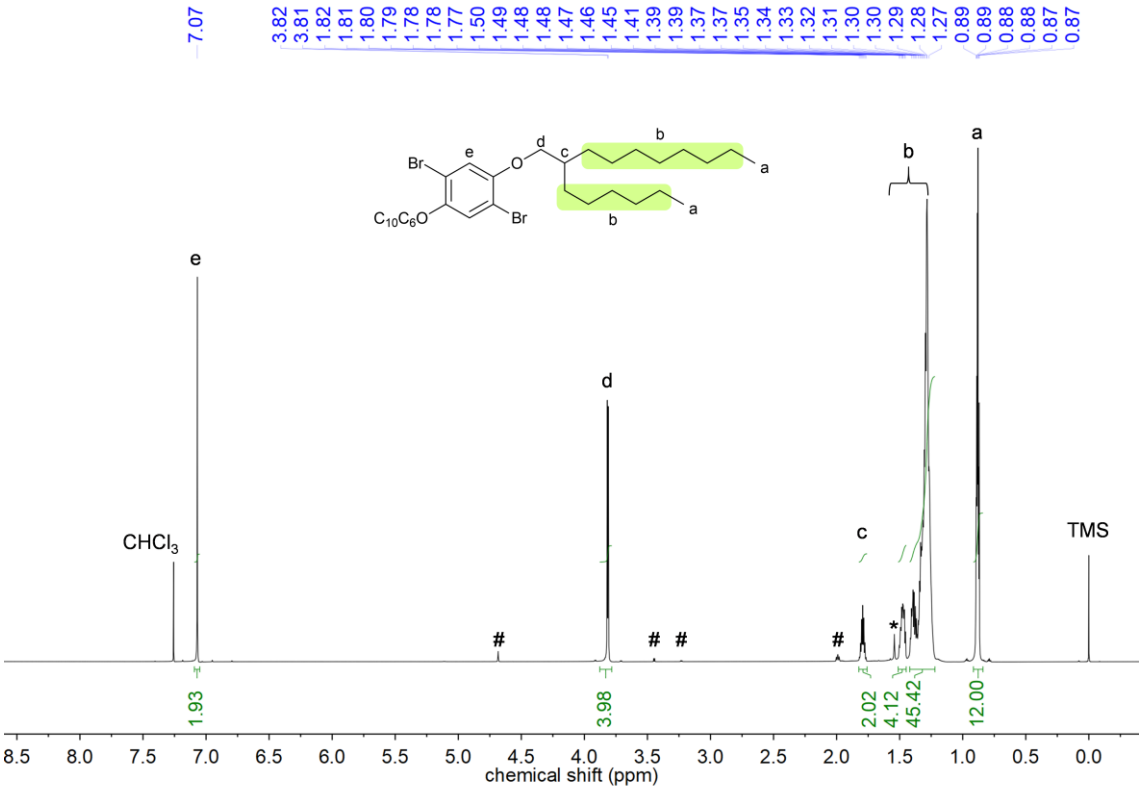

^{1}H NMR (700 MHz) spectrum of **3**. The asterisk represents residual water. The hashes represent impurity.

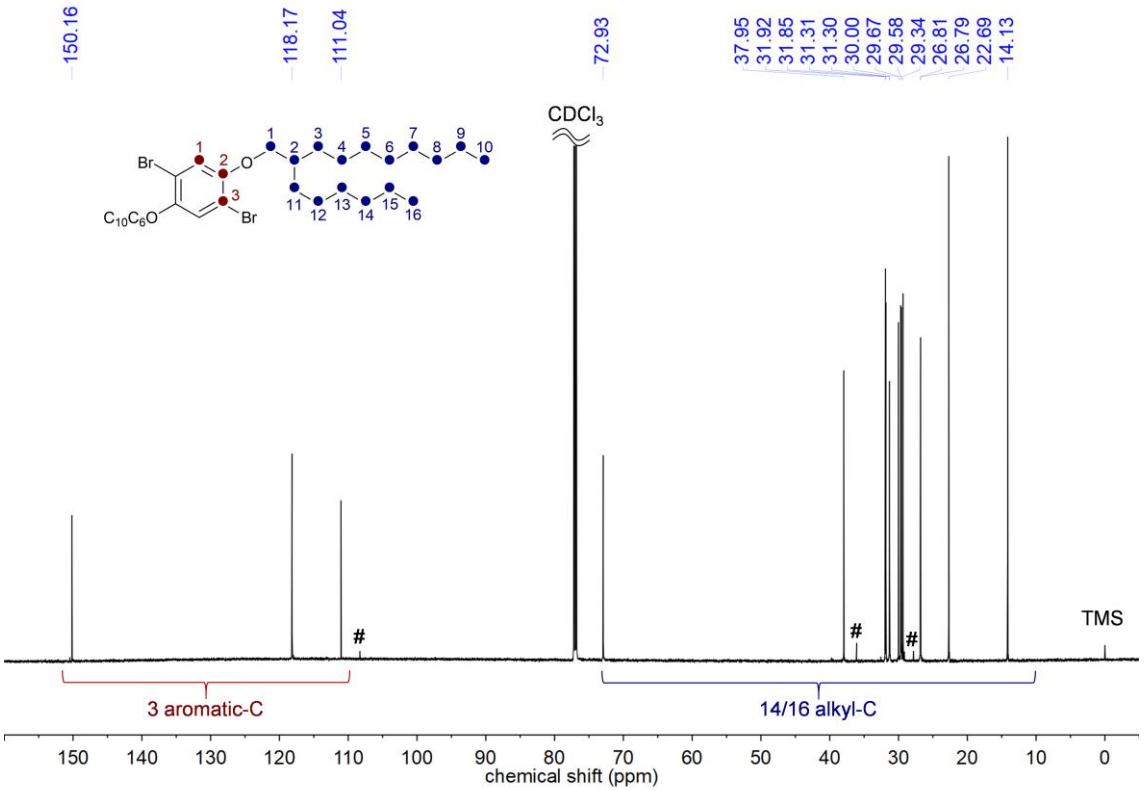

^{13}C NMR (176 MHz) spectrum of **3**. The hashes represent impurity.

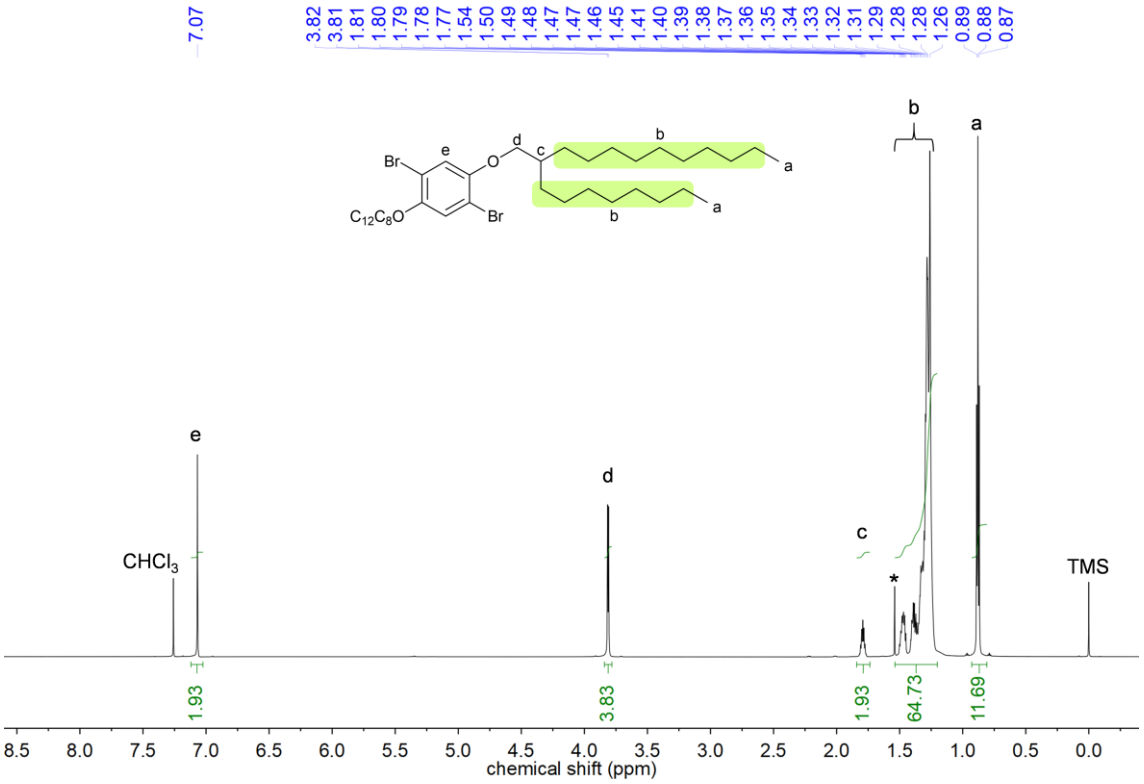

^{1}H NMR (700 MHz) spectrum of **4**. The asterisk represents residual water.

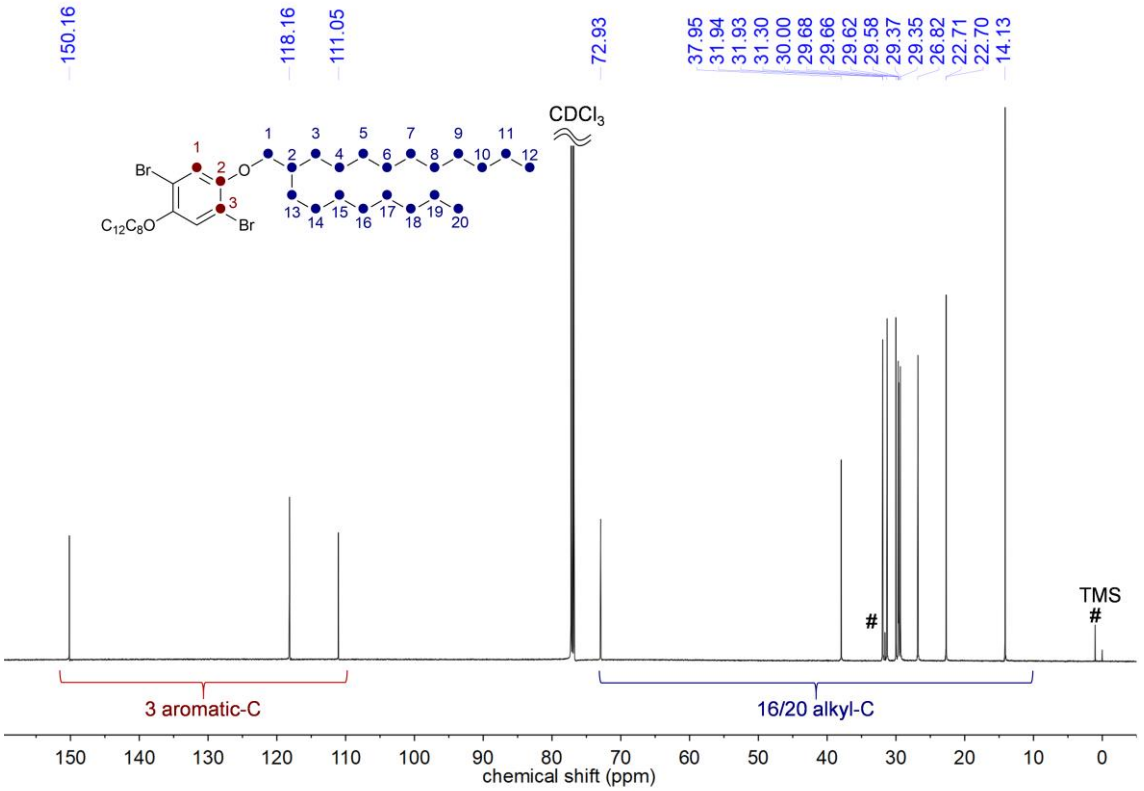

^{13}C NMR (176 MHz) spectrum of **4**. The hashes represent impurity.

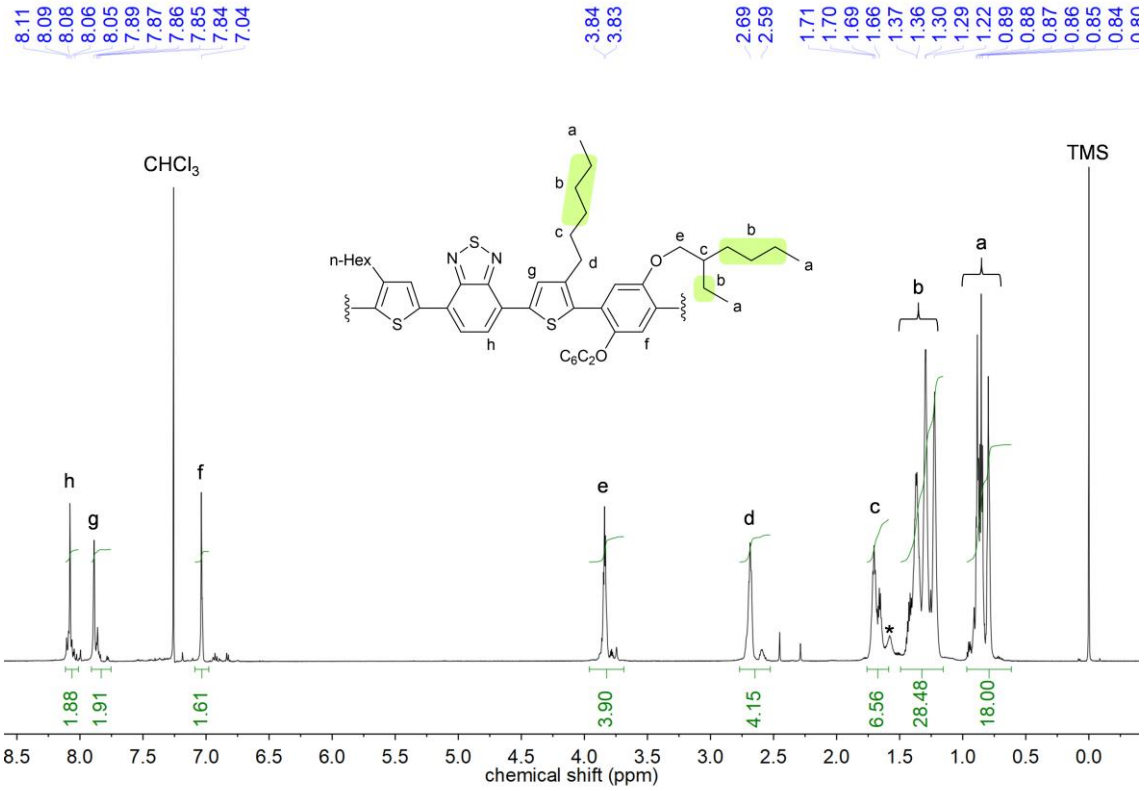

^{1}H NMR (700 MHz) spectrum of **P1**. The asterisk represents residual water.

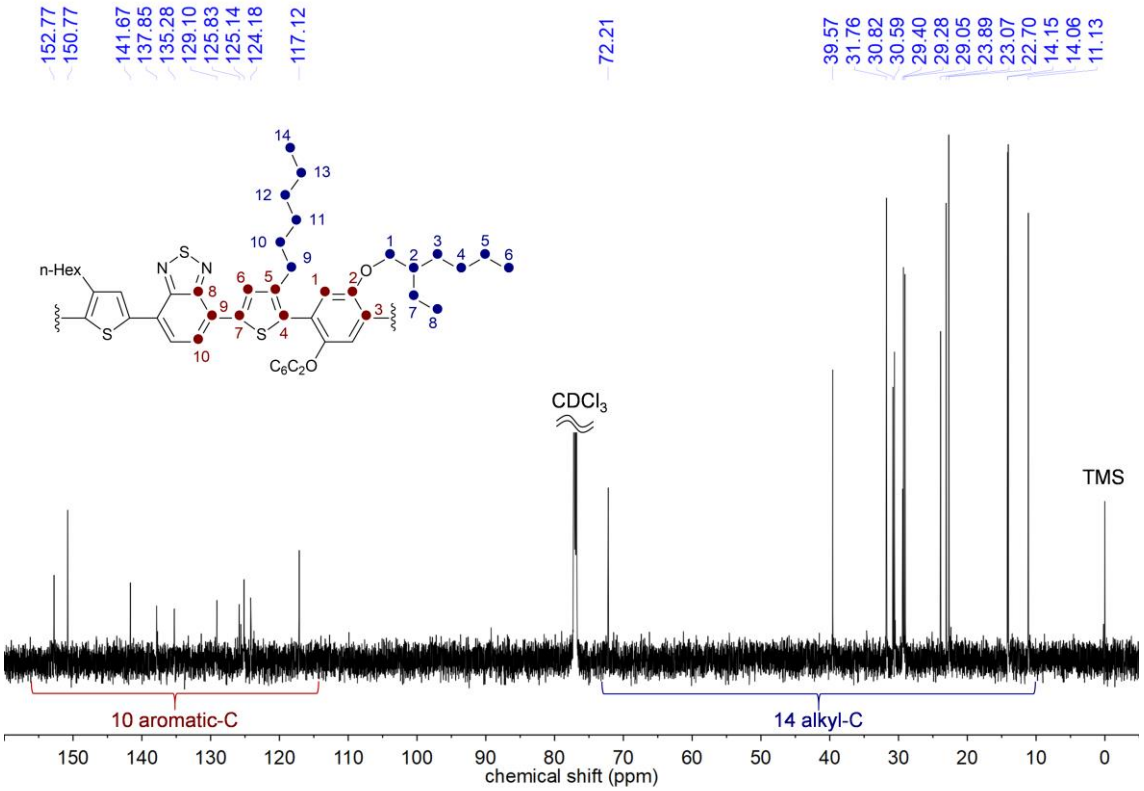

^{13}C NMR (176 MHz) spectrum of **P1**.

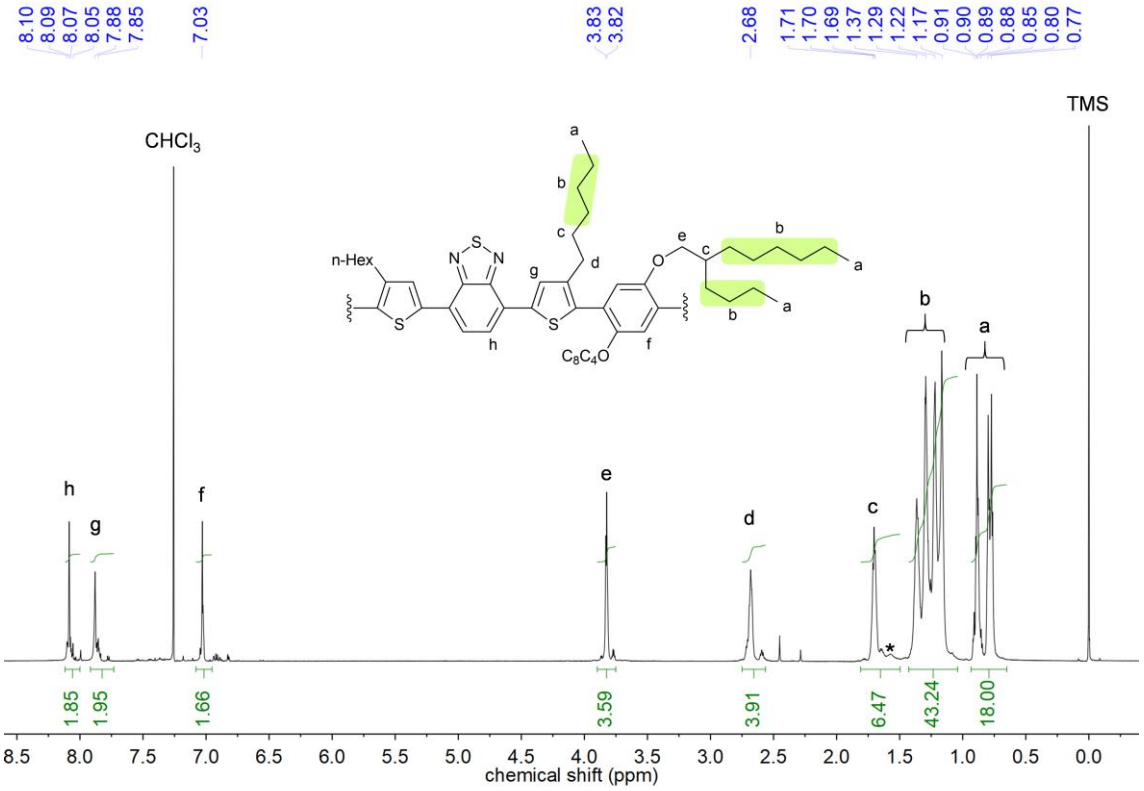

^{1}H NMR (700 MHz) spectrum of **P2**. The asterisk represents residual water.

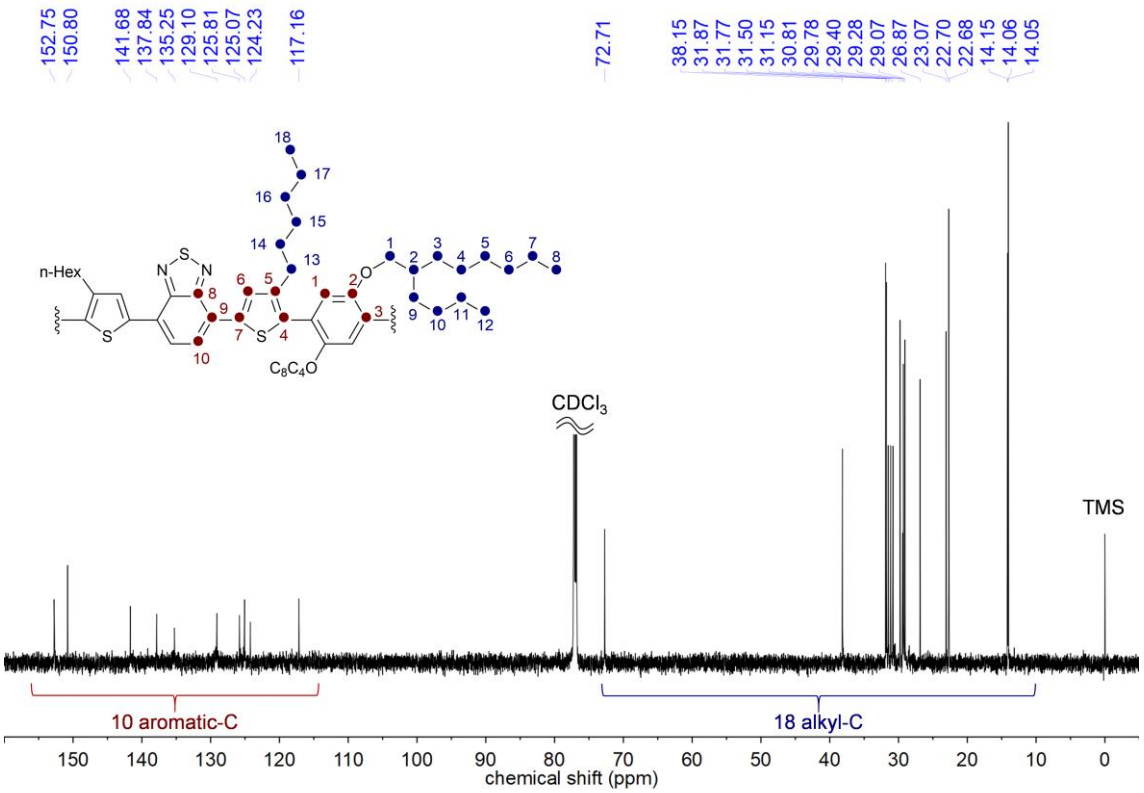

^{13}C NMR (176 MHz) spectrum of **P2**.

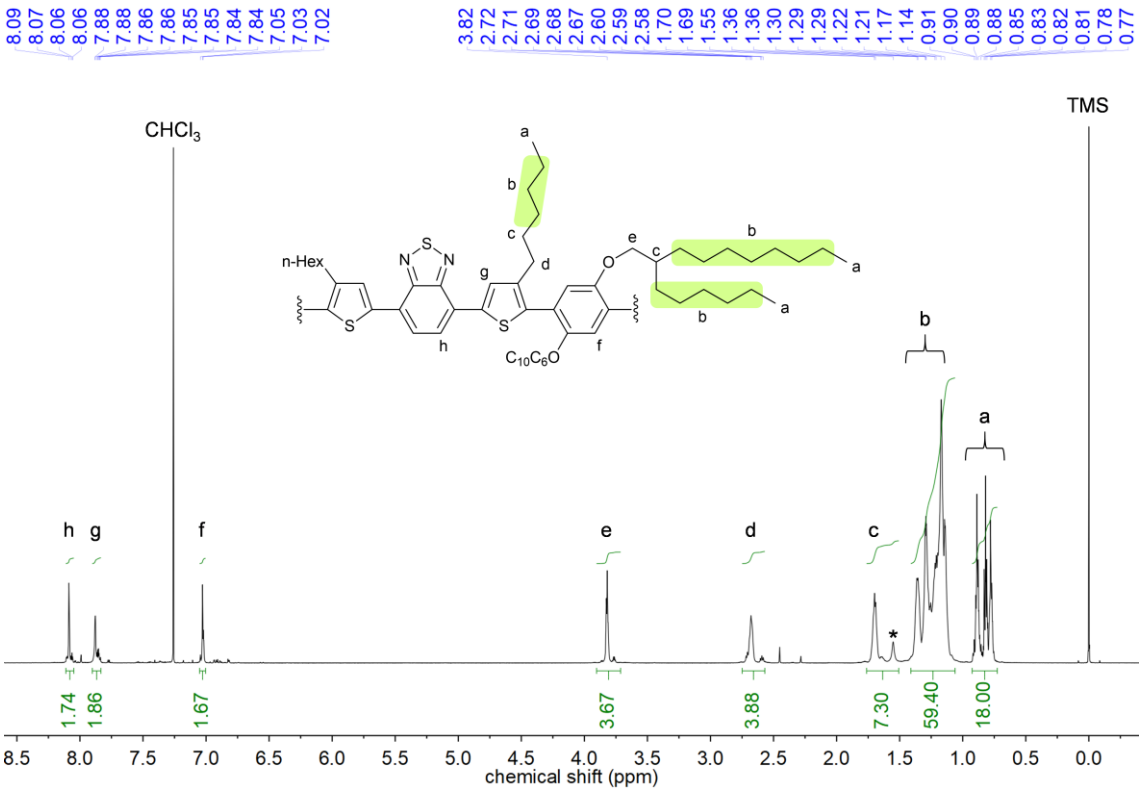

^{1}H NMR (700 MHz) spectrum of **P3**. The asterisk represents residual water.

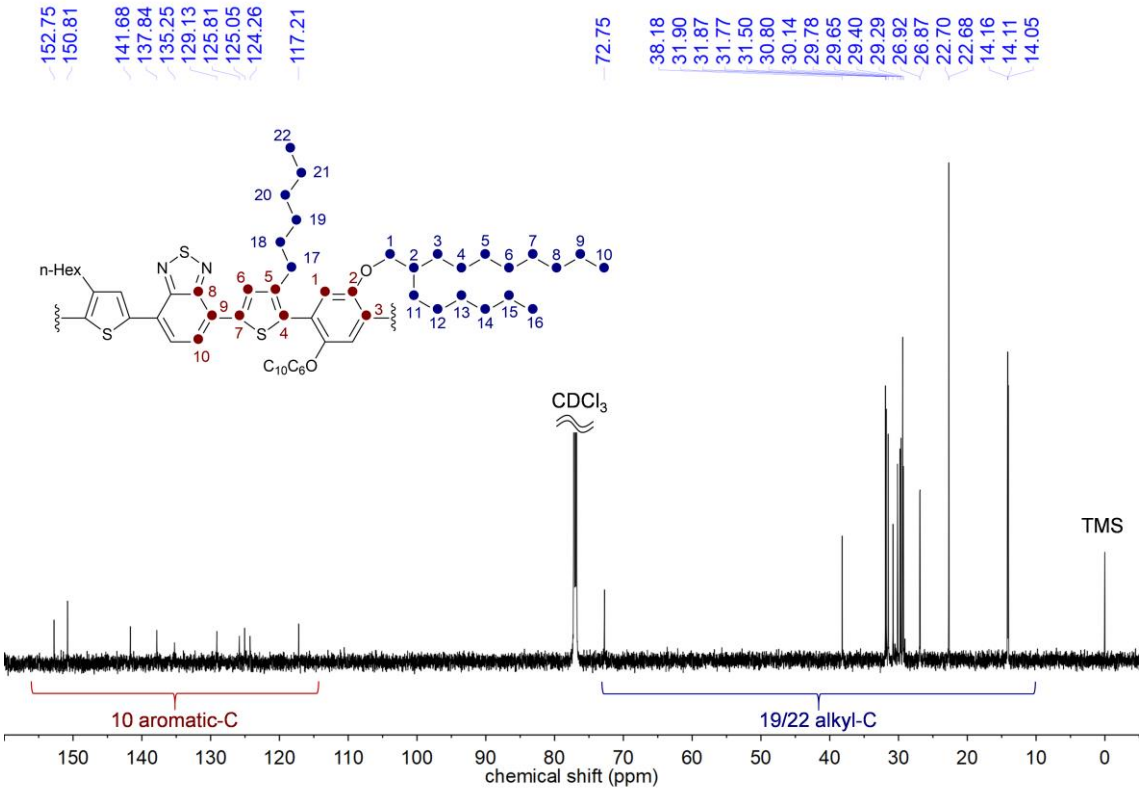

^{13}C NMR (176 MHz) spectrum of **P3**.

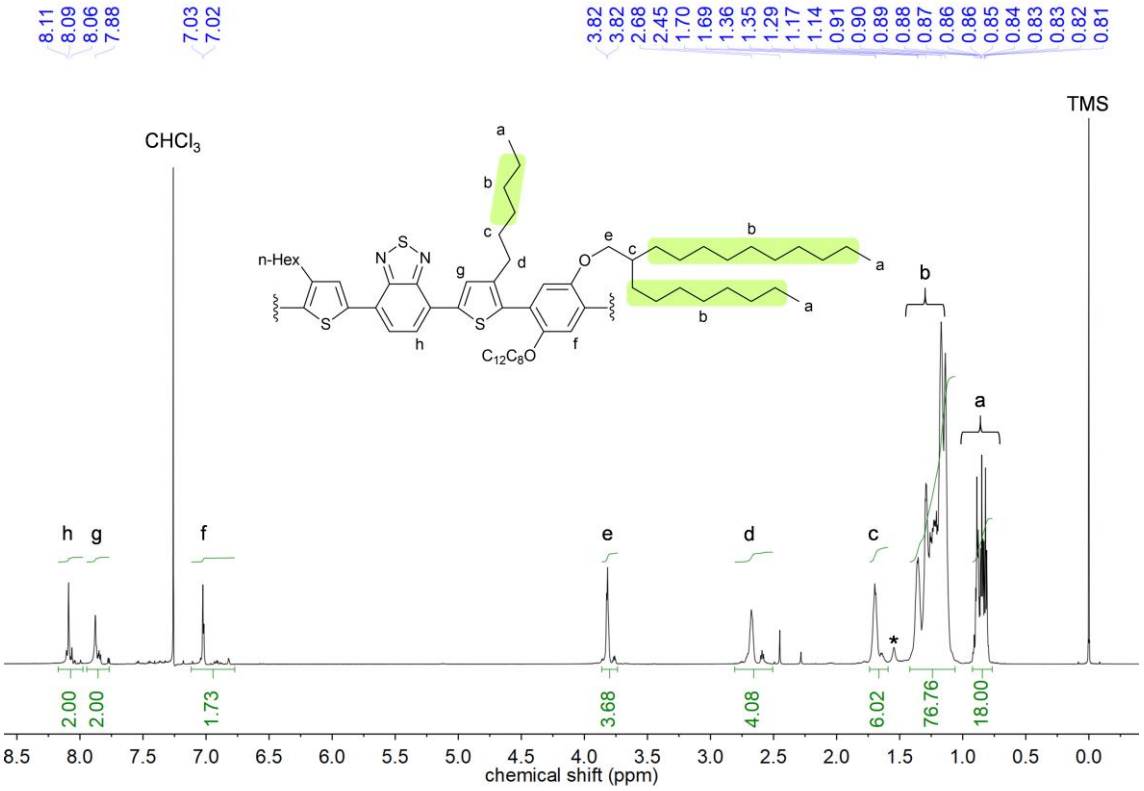

^{1}H NMR (700 MHz) spectrum of **P4**. The asterisk represents residual water.

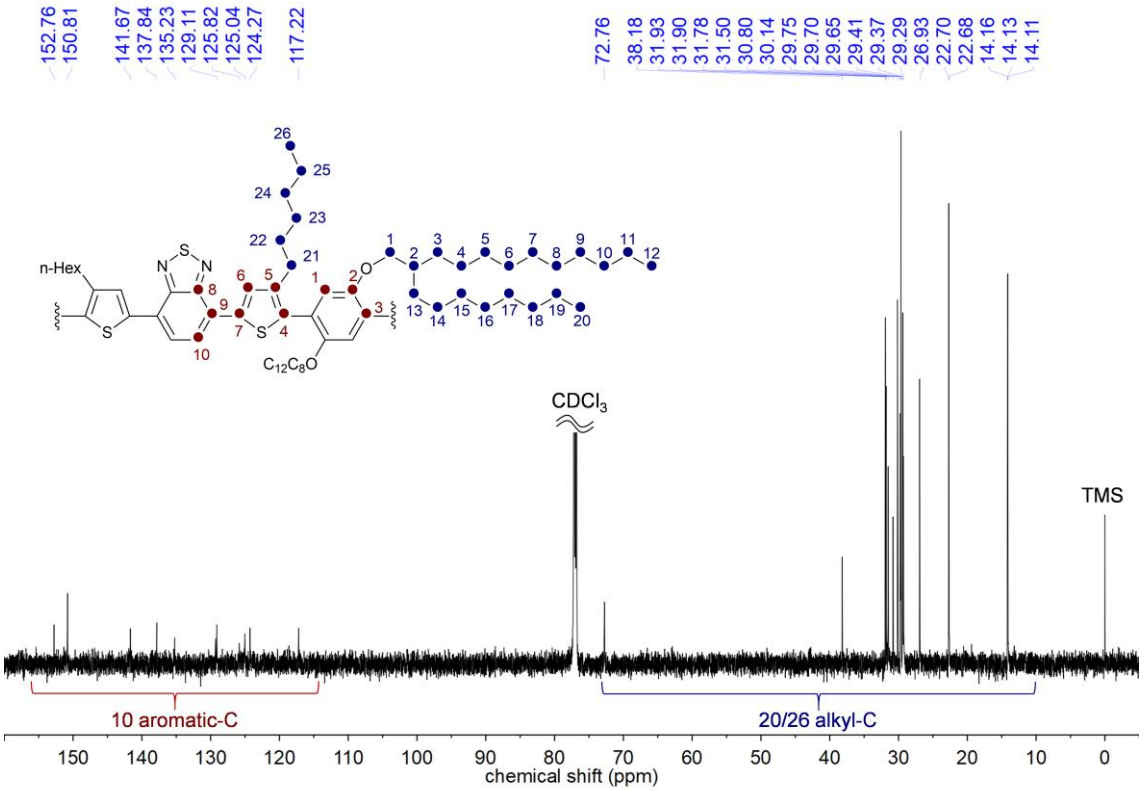

^{13}C NMR (176 MHz) spectrum of **P4**.

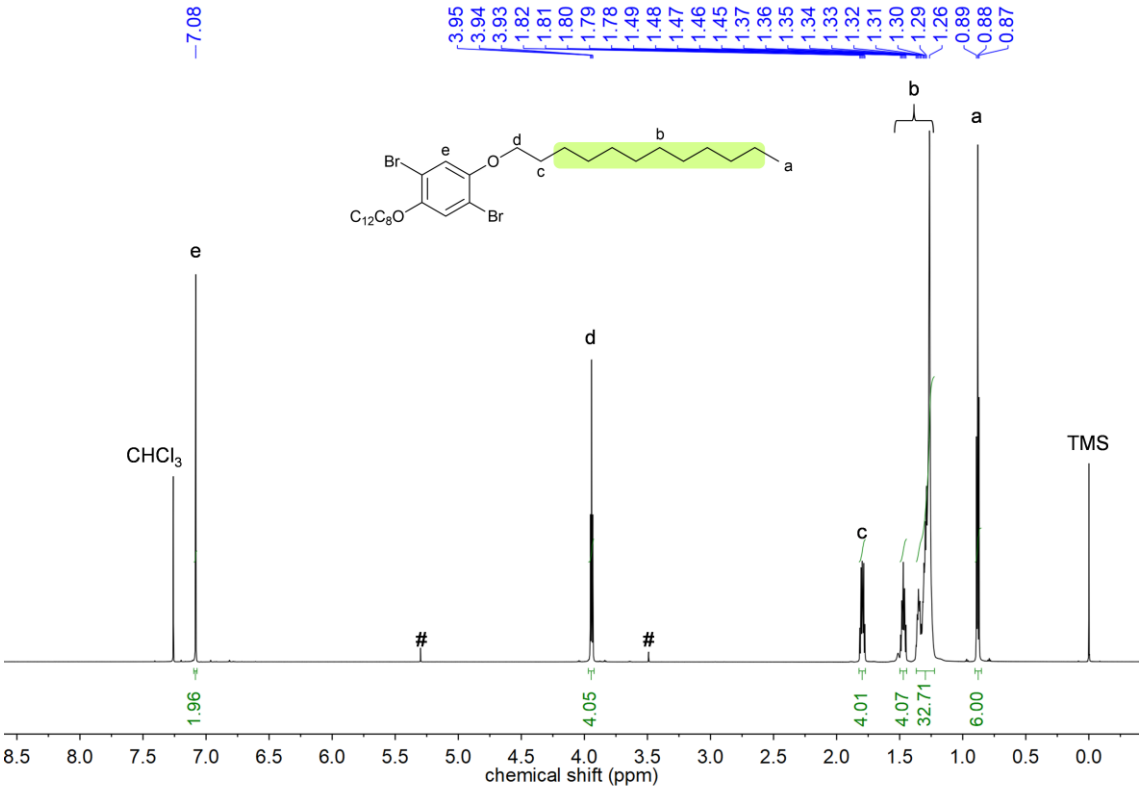

^{1}H NMR (700 MHz) spectrum of 1,4-dibromo-2,5-bis(dodecyloxy)benzene.

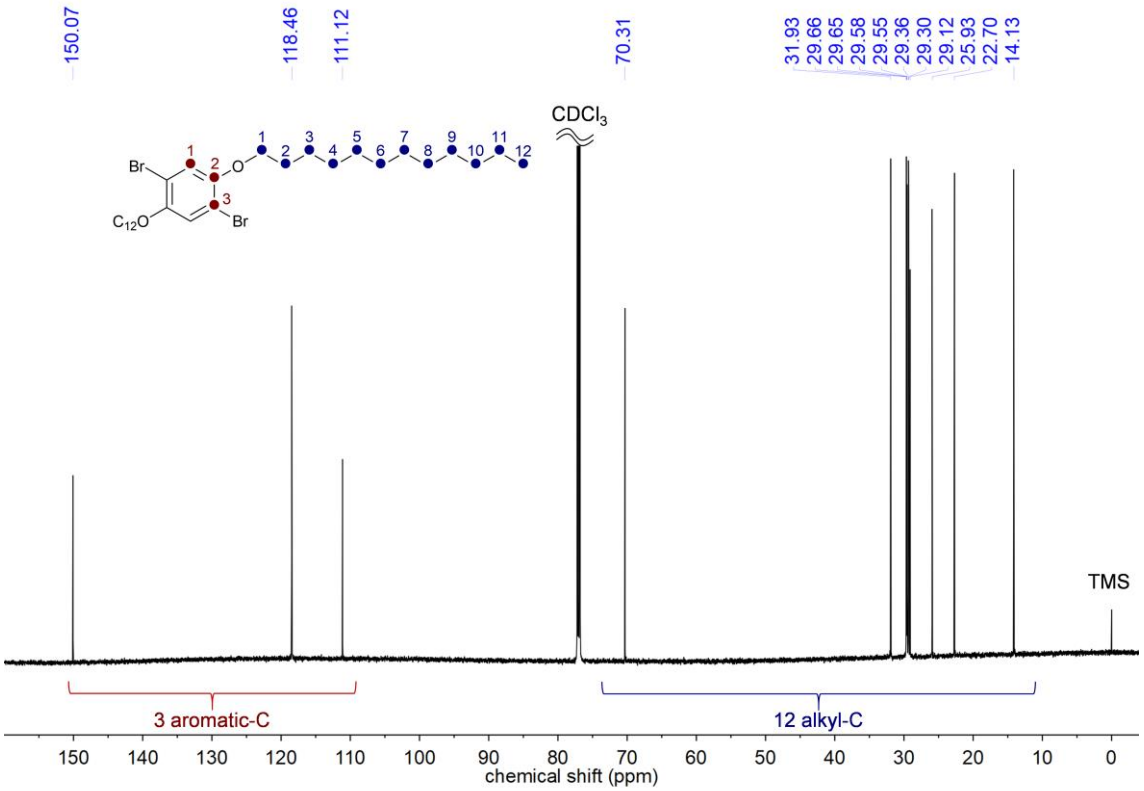

^{13}C NMR (176 MHz) spectrum of 1,4-dibromo-2,5-bis(dodecyloxy)benzene.

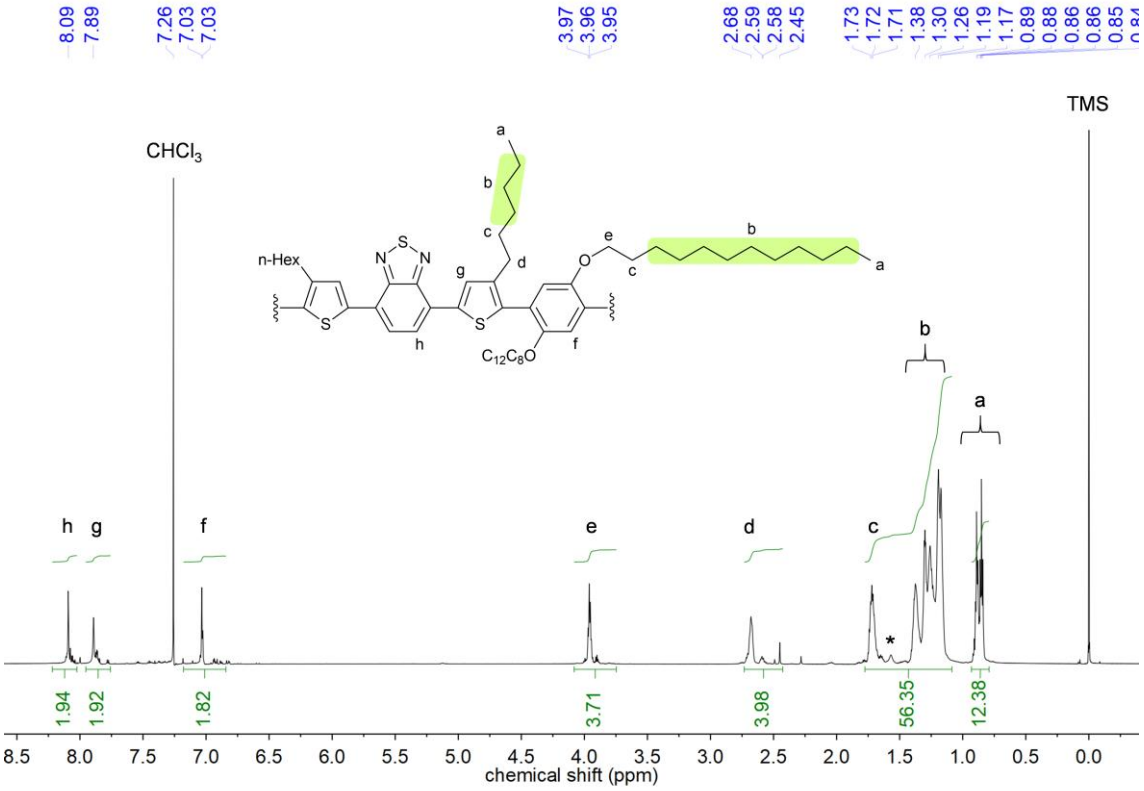

^{1}H NMR (700 MHz) spectrum of *n*-dodecyl analogue. The asterisk represents residual water.

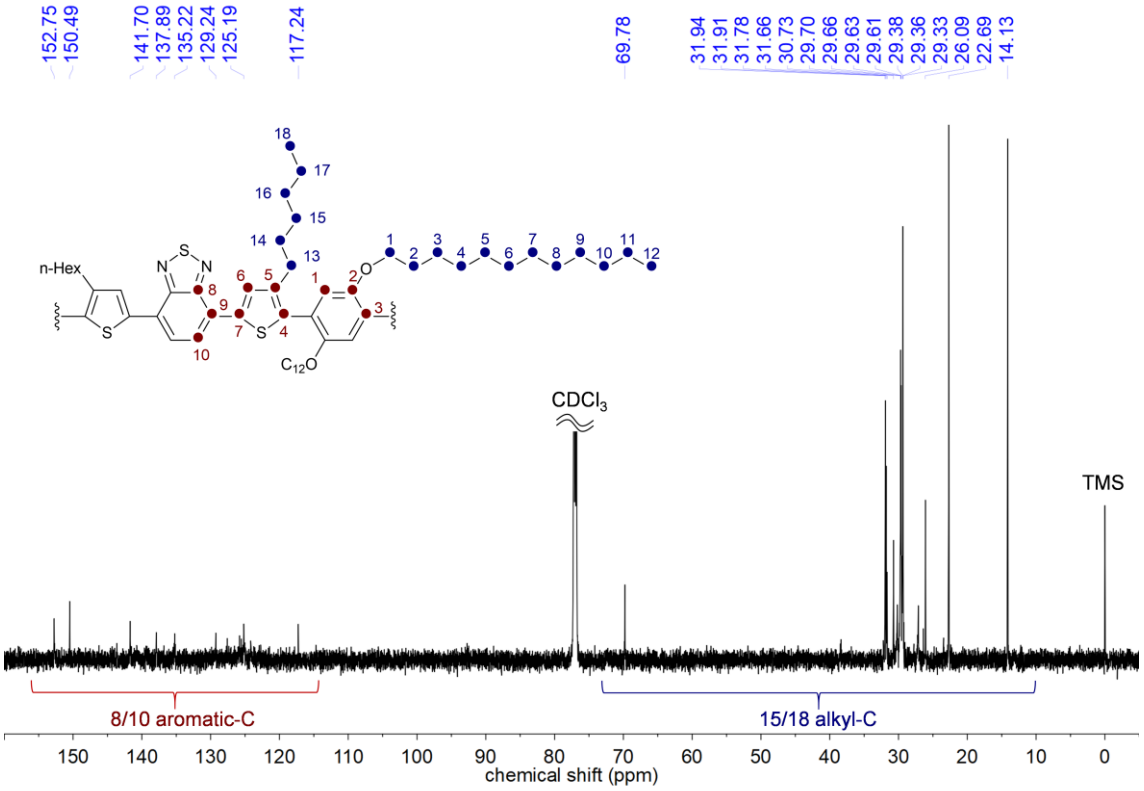

^{13}C NMR (176 MHz) spectrum of *n*-dodecyl analogue.